Dipolar model for collisional energy transfer between dark and radiating excited electronic states: CaO(A′1Π, a 3Π) +N2OCaO(A 1Σ+)+N2O

Millard H. Alexander

Articles you may be interested in

Electronic energy transfer on CaO surfaces
J. Chem. Phys. **129**, 124704 (2008); 10.1063/1.2980049

The electronic structure of CaO. II. An MCSCF/CI treatment of the lowlying 1Σ+ and 1Π states
J. Chem. Phys. **77**, 5573 (1982); 10.1063/1.443763

Model studies of the kinetics of collisional population transfer between dark and radiating excited electronic states: CaO(A′1Π)+N2OCaO(A 1Σ+)+N2O
J. Chem. Phys. **77**, 839 (1982); 10.1063/1.443900

A study of the reactions Ca(1 S,3 P 0, and 1 D)+N2O under singlecollision conditions and at higher pressures: Chemiluminescence cross sections, photon yields, and collisional energy transfer in CaO* by N2O
J. Chem. Phys. **74**, 6178 (1981); 10.1063/1.441008

Electron excitation of the E 3Σ g + state of N2 and subsequent collisional deactivation and energy transfer to the C 3Π u state
J. Chem. Phys. **65**, 2616 (1976); 10.1063/1.433449

Dipolar model for collisional energy transfer between dark and radiating excited electronic states: CaO($A'\,^1\Pi$, $a\,^3\Pi$) + N₂O ⇌ CaO($A\,^1\Sigma^+$) + N₂O

Millard H. Alexander

Department of Chemistry, University of Maryland, College Park, Maryland 20742
(Received 27 April 1981; accepted 21 September 1981)

Experimental evidence indicates that collisional transfer between low-lying excited electronic states occurs readily in a wide variety of diatomic molecules, in particular the alkaline earth oxides. We present here a model for this process, based on the long-range coupling of a permanent dipole of a polar collision partner and a transition dipole between the electronic states of the molecule of interest. We specifically investigate how spin–orbit or orbit–rotation mixing of two Born–Oppenheimer states can lead to substantial transition dipoles between the eigenfunctions of the full Hamiltonian for a diatomic molecule. The collision dynamics are treated within the time-dependent Born approximation, modified to ensure statistical microreversibility. A formulation in terms of spherical tensors facilitates the application of known techniques to the collision of molecules whose eigenfunctions are linear combinations of states of nonzero electronic angular momentum. We describe the calculation of cross sections and rate constants for transfer within and between the rotational manifolds of selected near resonant vibrational levels of the (nominally) $A\,^1\Sigma^+$, $A'\,^1\Pi$, and $a\,^3\Pi$ states of CaO, as well as for transfer between the Λ-doubling components of the $A'\,^1\Pi$ state. The rate constants for electronic state transfer are substantial ($> 1 \times 10^{-10}\,\mathrm{cm^3/molecule\,s}$) over a wide range of rotational levels in the neighborhood of the various isoenergetic points, where, for a particular pair of vibrational quantum numbers, the rotational ladders cross. No evidence is seen for a continuous transfer rate, independent of rotational quantum number, even at high values of J.

I. INTRODUCTION

Recently, there has been considerable experimental interest[1-20] in reactions of alkaline earth atoms with molecular oxidants. Often the exoergicities are large enough to allow formation of the alkaline earth oxide products in one or more electronically excited states. For each alkaline earth oxide, there exists four low-lying excited states $^{1,3}\Pi$ and $^{1,3}\Sigma^+$, only one of which, the $A\,^1\Sigma^+$ state, has a strong transition moment to the ground state ($X\,^1\Sigma^+$).[21-23] A sizeable body of experimental evidence[2,7,8,18-20] indicates that the total chemiluminescence yield increases with increasing pressure of the oxidant gas (typically N₂O or NO₂). This suggests that inelastic collisions, subsequent to the initial formation of products, can act to transfer population from one or more of the dark excited states ($^{1,3}\Pi$, $^3\Sigma^+$) into the radiating $A\,^1\Sigma^+$ state.[9,11,18] For CaO, SrO, and BaO all four excited states are nearly isoenergetic,[21] so it would not be unreasonable to expect the occurrence of fast near-resonant processes. There has been some speculation that non-Born–Oppenheimer perturbations (spin–orbit, orbit–rotation) are involved.[11,20] Evidence for a similar type of energy transfer has been inferred from experiments on other metallic oxides[24,25] and in the CN, CO⁺, and N₂⁺ molecules.[26,27]

In this paper we develop a kinetic model for collisional energy transfer between two rotational manifolds corresponding to vibrational levels of two different Born–Oppenheimer electronic states of a polar molecule which are nearly isoenergetic and which are coupled by small perturbations. The resulting mixing of the Born–Oppenheimer states leads to appreciable transition dipoles between the eigenfunctions of the full Hamiltonian for the isolated molecule. The collisional coupling between this transition dipole and the dipole moment of a polar target will lead to inelastic transitions between rotational manifolds of different electronic states. This energy transfer process is similar to the efficient rotational relaxation which occurs due to the coupling between the permanent dipole moment in a given electronic state and the dipole moment of a collision partner.

If one of the electronic states is nonradiating, then the net effect of inelastic collisions will be the transfer of population from the dark to the radiating state. This dipole–dipole energy transfer between two near-resonant excited states of the same molecule, which can be represented schematically by the equation

$$AB^* + CD \rightarrow AB^{**} + CD , \qquad (1)$$

should not be confused with a similar process, wherein electronic excitation is transferred from one molecule to another, namely,

$$AB^* + CD \rightarrow AB + CD^* . \qquad (2)$$

Several theoretical treatments of the latter process have appeared in the literature[28-31] for systems where dipole–dipole coupling provides the mechanism for energy transfer.

In the present paper we consider the particular case of population transfer from the $A'\,^1\Pi$ and $a\,^3\Pi$ states of CaO to the radiating $A\,^1\Sigma^+$ state. Our interest in this system is motivated by the recent molecular beam study by Irvin and Dagdigian[7,8] of the pressure dependence of the CaO $A\,^1\Sigma^+ \rightarrow X\,^1\Sigma^+$ chemiluminescence subsequent to the reaction of Ca(^3P, ^1D) atoms with N₂O. The organization of this paper is as follows: In the next section we discuss the mixing between the rotational manifolds of the Born–Oppenheimer $A\,^1\Sigma^+$ and $A'\,^1\Pi$ states and $a\,^3\Pi$ and $A\,^1\Sigma^+$ states. In the former case, the mixing arises from the orbit–rotation perturbation, and in the later case from the spin–orbit perturbation. The mixing affects only one of the Λ-doubled components and, in the case of the

© 1982 American Institute of Physics 429

$^3\Pi$ state, only one of the spin–orbit components. [21,32,33] As we shall see, it is only these components which are strongly dipole coupled to the $A\,^1\Sigma^+$ state. Expressions are derived in Sec. III for matrix elements of the dipole operator between the eigenstates of the full Hamiltonian.

Since cross sections for dipole–dipole processes are known to be large whenever the inelastic energy gaps are small, as is the case in the present application, it might be expected that the dominant channel for population transfer into the $A\,^1\Sigma^+$ state will occur via these dipole-coupled Π-state components. Within a formalism based on spherical tensors the standard impact parameter Born approximation[34–37] can be easily adapted to the determination of cross sections for transitions between the perturbed Born–Oppenheimer states. This is described in Sec. IV. The work presented here differs from that of Chiu[29] in that we use the time-dependent Born approximation. A correction to ensure microreversibility can be made identical to the one we have recently introduced. [38] The application to the determination of cross sections and thermal rate constants for energy transfer in the CaO system is described in Sec. V and the results presented in Sec. VI. A brief discussion follows.

Fundamentally, the present paper represents an attempt to treat the dynamics of collisional energy transfer between molecular states of nonzero electronic angular momentum. It is thus similar in spirit to previous papers dealing with energy transfer in the NO molecule[28,29] and, more recently, with transfer between the Λ-doubling levels of the ground $^2\Pi$ state of OH. [39–41] The particular attention given here to dipole-coupled inelastic collisions between two different electronic states represents an extension of our earlier work[42] on energy transfer between the $A\,^3\Sigma_u^+$, $B\,^3\Pi_g$, and $W\,^3\Delta_u$ states of N_2.

II. NON-BORN–OPPENHEIMER MIXING OF DARK AND LIGHT PRODUCT STATES

In Hund's case (a) an eigenstate of a diatomic molecule can be specified by the quantum numbers J, Ω, M, v, S, Λ, and Σ. [43,44] The quantity J is the total angular momentum with projections along space- and molecule-fixed axis systems of M and Ω, respectively. Here v denotes the vibrational quantum number, S the total spin, and Λ and Σ denote the projections along the molecular axis of the electronic and spin angular momenta, respectively. The corresponding total wave function may be written as the product of the wave function for the rotation of the molecule in space multiplied by a wave function which describes the electronic and vibrational motion in the nonrotating molecule, namely, [43,44]

$$|J\Omega MvS\Lambda\Sigma\rangle = |J\Omega M\rangle\,|vS\Omega\Sigma\rangle\ . \tag{3}$$

Explicit expressions for the product wave functions are given in the Appendix. Often we will replace the quantum numbers $S\Lambda\Sigma$ by the corresponding electronic term symbols.

Consider $^1\Sigma^+(S=\Sigma=\Lambda=0)$, $^1\Pi(S=\Sigma=0,\ \Lambda=\pm1)$, and $^3\Pi(S=1,\ \Sigma=0,\ \pm1,\ \Lambda=\pm1)$ states which are eigenfunctions of the Born–Oppenheimer Hamiltonian. We shall use the definite parity Π states, which are linear com-

binations of the individual components, namely, for $^1\Pi$, [44]

$$|JMv_\Pi\,^1\Pi_{P_\pm}\rangle = 2^{-1/2}[\,|J,\Omega=1,MvS,\Lambda=1,\Sigma=0\rangle$$
$$\pm\,|J,\Omega=-1,MvS,\Lambda=-1,\Sigma=0\rangle]\ , \tag{4}$$

and, for $^3\Pi_{|\Omega|=0}$,

$$|JMv_\Pi\,^3\Pi_{0_{P_\pm}}\rangle = 2^{-1/2}[\,|J\Omega MvS,\Lambda=1,\Sigma=-1\rangle$$
$$\pm\,|J\Omega MvS,\Lambda=-1,\Sigma=+1\rangle]\ . \tag{5}$$

The linear combinations corresponding to the p_+ parity label are designated Π_e and those corresponding to p_- are designated Π_f. [33] Expressions for the $|\Omega|=1$ and $|\Omega|=2$ components of the $^3\Pi$ state can be written in a similar fashion.

The full molecular Hamiltonian includes a weak Coriolis orbit–rotation term which will mix the $^1\Sigma^+$ and $^1\Pi_e$ Born–Oppenheimer wave functions. The matrix element of this orbit–rotation term is diagonal in the total rotational angular momentum J and its space fixed projection M, and is given by[21,32]

$$\langle JMv_\Pi\,^1\Pi_e|H_{OR}|JMv_\Sigma\,^1\Sigma^+\rangle$$
$$= -[2J(J+1)]^{1/2}\,b\,\langle v_\Pi|B|v_\Sigma\rangle\ , \tag{6}$$

where, for simplicity, we have suppressed the $\Omega=0$ index for the $^1\Sigma^+$ state. Here $\langle v_\Pi|B|v_\Sigma\rangle$ denotes the off-diagonal element of the moment of inertia $(B=\hbar^2/2\mu r^2)$, and b is a strength constant, whose magnitude can be determined spectroscopically and which is defined as the matrix element of the electronic orbital angular momentum operator L_+, namely, [32,43]

$$b = \langle\,^1\Pi,\Lambda=1|L_+|^1\Sigma^+\rangle\ . \tag{7}$$

We have kept the notation of Field[25] but with the phase convention of Gottscho, Koffend, and Field. [32] Similarly, the $\Omega=0$, e component of a $^3\Pi$ state will be mixed with a $^1\Sigma^+$ state by the spin–orbit term in the full Hamiltonian. The matrix element takes the form[21,32]

$$\langle JMv_\Pi\,^3\Pi_{0e}|H_{SO}|JMv_\Sigma\,^1\Sigma^+\rangle = \tfrac{1}{2}a_+\langle v_\Pi|v_\Sigma\rangle\ , \tag{8}$$

where a_+ is a strength constant and $\langle v_\Pi|v_\Sigma\rangle$ is the vibrational overlap.

For the first excited states of the alkaline earth oxides[23] ($A\,^1\Sigma^+$, $A'\,^1\Pi$, $a\,^3\Pi$) the couplings are relatively small in magnitude[21] ($\sim 10\ cm^{-1}$), so that the mixing between the Π and Σ Born–Oppenheimer wave functions will be significant only for Σ and Π vibrational levels which are nearly isoenergetic. Thus, the wave functions and energies of the full Hamiltonian differ significantly from the Born–Oppenheimer wave functions and energies only in the region of these isoenergetic points. From the existence of spectral perturbations we know that for each of the low-lying vibrational levels of the $A\,^1\Sigma^+$ state in CaO, SrO, and BaO an energy match exists with several vibrational levels of both the $A'\,^1\Pi$ and $a\,^3\Pi$ ($b\,^3\Pi$ in the case of BaO[23]) states. [21] As an illustration, Fig. 1 displays the energy dependence of the $v_\Sigma=0$–4 and $v_\Pi=5$–11 levels of the (nominally) $A\,^1\Sigma^+$ and the (nominally) $A'\,^1\Pi_e$ states of CaO as a function of $J(J+1)$. The isoenergetic points are indicated. [45] There exists one crossing per pair of $^1\Sigma^+$ and $^1\Pi_e$ vibrational
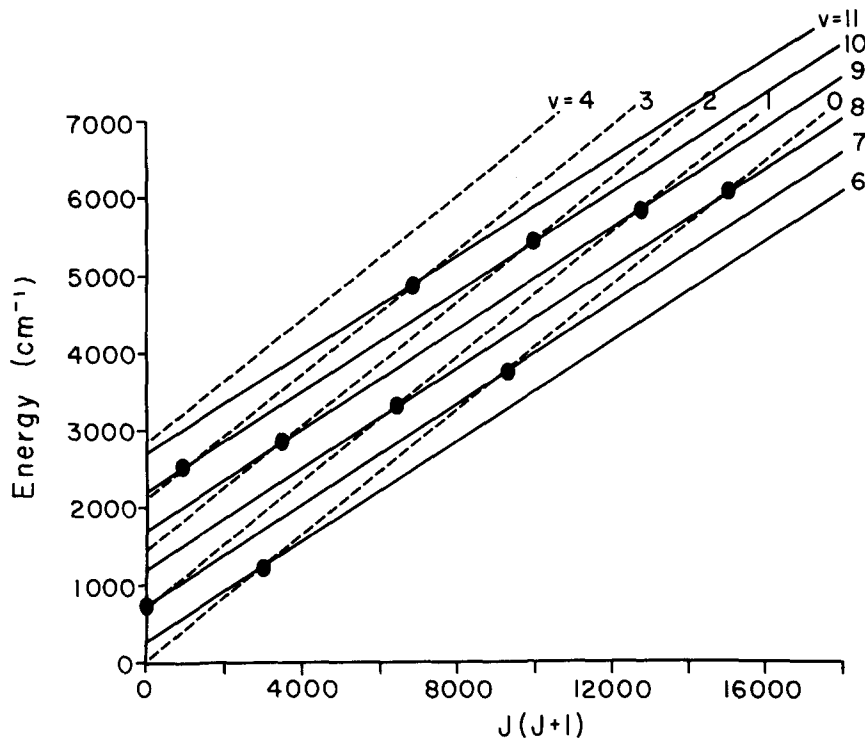
FIG. 1. Dependence on rotational quantum number of the energies of the v_Σ =0–4 (dashed lines) and v_Π =6–11 (solid lines) rotational manifolds of the Born–Oppenheimer $A\,^1\Sigma^+$ and $A'\,^1\Pi$ states of CaO (see Ref. 45). The isoenergetic points, where the maximum non-Born–Oppenheimer mixing will occur, are marked by filled circles.

levels, and, similarly but not shown, for the $^1\Sigma^+$, $^3\Pi_{0e}$ pairs.

Consider then the two rotational manifolds corresponding to one of these particular vibrational pairs. The relative energy of the two Born–Oppenheimer levels with a given value of J are[43,44]

$$\Delta E_J = E_{v_\Sigma,J} - E_{v_\Pi,J} = T_{v_\Sigma,v_\Pi} + J(J+1)(B_{v_\Sigma} - B_{v_\Pi}) \pm B_{v_\Pi}, \tag{9}$$

where the positive sign refers to the $^1\Pi_e$ state and the negative sign to the $^3\Pi_{0e}$ state, and where T_{v_Σ,v_Π} is the vibronic energy difference. Since for CaO, SrO, and BaO the $A\,^1\Sigma^+$ state has a larger rotational constant than the Π states,[21] significant coupling will occur only if the vibronic energy difference is negative, so that the two electronic states will become exactly degenerate when the rotational quantum number attains the value, in the semiclassical limit,

$$J_{\mathrm{cross}} = \left[-(T_{v_\Sigma,v_\Pi} \pm B_{v_\Pi})/(B_{v_\Sigma-v_\Pi}) \right]^{1/2} - \tfrac{1}{2}. \tag{10}$$

For rotational quantum numbers less than J_{cross} the rotational levels of the A state will lie below the comparable $^1\Pi$ or $^3\Pi$ levels, with a reversal occurring for $J > J_{\mathrm{cross}}$.

As stated above, the presence of small non-Born–Oppenheimer terms in the full Hamiltonian will result in a mixing of the two rotational manifolds. For simplicity we shall treat separately the mixing between the $^1\Sigma^+$ state and each Π state; a discussion of the more complicated three-manifold case, involving both the $^1\Pi_e$ and $^3\Pi_{0e}$ states, will be deferred until Sec. VII. Our treatment of this perturbation induced mixing is similar in spirit to the treatments by Field, Pruett, Gole, and their collaborators.[24,46,47] The eigenfunctions of the full Hamiltonian will be denoted as $|JM+\rangle$

and $|JM-\rangle$, respectively, where, for the mixing between the $^1\Sigma^+$ and $^1\Pi_e$ states,

$$|JM\pm\rangle = C_J^\pm |JMv_\Sigma\,^1\Sigma^+\rangle + D_J^\pm |JMv_\Pi\,^1\Pi_e\rangle, \tag{11}$$

and, for the mixing between the $^1\Sigma^+$ and $^3\Pi_{0e}$ states,

$$|JM\pm\rangle = F_J^\pm |JMv_\Sigma\,^1\Sigma^+\rangle + G_J^\pm |JMv_\Pi\,^3\Pi_{0e}\rangle. \tag{12}$$

For the $^1\Sigma-^1\Pi_e$ mixing the spin S and its projection Σ are still good quantum numbers for the $|JM\pm\rangle$ states. Similarly, for the $^1\Sigma-^3\Pi_{0e}$ mixing the projection Ω remains a good quantum number for the $|JM\pm\rangle$ states. For simplicity, these indices will be suppressed except where explicitly needed.

The mixing coefficients $C^\pm$ and $D^\pm$ are easily obtained by diagonalization of a 2×2 matrix with off-diagonal elements given by Eqs. (6) and (8) and are related by

$$D_J^\pm = (1 - C_J^{\pm 2})^{1/2}, \tag{13a}$$

$$C_J^- = D_J^+, \tag{13b}$$

and

$$D_J^- = -C_J^+. \tag{13c}$$

The $F^\pm$ and $G^\pm$ coefficients satisfy identical relationships. The coefficients will be real, because the matrix elements are real. We will associate, arbitrarily, the minus sign with the higher energy. The corresponding eigenvalues will be denoted as $E_J^\pm$. Except very near the isoenergetic point the predominant character of the full eigenfunctions will be either $^1\Sigma^+(|C_J| > |D_J|, |F_J| > |G_J|)$ or $\Pi(|C_J| < |D_J|, |F_J| < |G_J|)$. As discussed above, we assume that the vibronic energy difference is negative, so that for values of J less than J_{cross} [Eq. (10)] the lower energy member of the pair will be predominantly $^1\Sigma^+(|C_J^+|, |F_J^+| > 0.5)$ and the higher energy member predominantly $\Pi(|C_J^-|, |F_J^-| < 0.5)$. A reversal

will occur when the total angular momentum becomes greater than J_{cross}. We will assume that the energies are measured with respect to the Born–Oppenheimer energy for the v_Σ, $J=0$ level of the $^1\Sigma^+$ state.

The reader should note that the $|JM\pm\rangle$ states [Eqs. (11) and (12)] are eigenfunctions of the full Hamiltonian for the diatomic molecule, so that the coefficients in Eqs. (11) and (12) do not show any time dependence, other than an overall phase factor $\exp(-iE_J^\pm t/\hbar)$ which is identical for both coefficients. The Born–Oppenheimer Hund's case (a) states should be thought of as basis functions for the full molecular Hamiltonian.

III. DIPOLE MATRIX ELEMENTS

In anticipation of the treatment of collisional energy transfer contained in the next section it is useful to consider expectation values of the electric dipole moment operator, defined by[48]

$$Q_{1m} = (4\pi/3)^{1/2} e \sum_i z_i r_i Y_{1m}(\theta_i, \phi_i) , \tag{14}$$

where e is the electronic charge and the sum is taken over all the particles in the molecule of charge z_i. In the Appendix, an expression is derived for the expectation value of a generalized multipole moment between two states defined by Eq. (3). From Eq. (A10) we see that the expectation value of the qth component, in a space-fixed axis system, of the electric dipole operator can be expressed in the factorized form

$$\langle J'\Omega'M'v'S'\Lambda'\Sigma' | Q_{1m} | J\Omega MvS\Lambda\Sigma \rangle = (-1)^{J'-M'}$$
$$\times \begin{pmatrix} J' & 1 & J \\ -M' & m & M \end{pmatrix} (J'\Omega'v'S'\Lambda'\Sigma' || Q_1 || J\Omega vS\Lambda\Sigma) , \tag{15}$$

where $(:::)$ is a $3j$ symbol.[49,50]

The reduced or double-bar matrix element in Eq. (15) follows from Eq. (A11), namely,

$$(J'\Omega'v'S'\Lambda'\Sigma' || Q_1 || J\Omega vS\Lambda\Sigma) = (-1)^{-J'-\Omega'}\delta(S,S')\delta(\Sigma,\Sigma')$$
$$\times \delta(J',1,J)Q_{v'v}^{1;\Lambda'-\Lambda}[(2J'+1)(2J+1)]^{1/2} \begin{pmatrix} J' & 1 & J \\ -\Omega' & \Lambda'-\Lambda & \Omega \end{pmatrix} , \tag{16}$$

when $\delta(i, j, k) = 1$ if i, j, and k satisfy the triangular condition, and is zero otherwise. As discussed in the Appendix, the quantity $Q_{v'v}^{1;\Lambda'-\Lambda}$ is the only nonvanishing molecule frame component of the expectation value of the electric dipole operator taken over the wave function of the nonrotating molecule, in other words

$$\langle v'S'\Lambda'\Sigma' | Q_{1q} | vS\Lambda\Sigma \rangle = \delta(S,S')\delta(\Sigma,\Sigma')\delta(q, \Lambda'-\Lambda)Q_{v'v}^{1;\Lambda'-\Lambda} . \tag{17}$$

The index q will refer to the molecule-fixed frame component of the electric dipole operator.

The factor in front of the reduced matrix element in Eq. (15) contains no dependence on the quantum numbers Ω, v, S, Λ, and Σ. Thus, the expectation value of the dipole moment operator can still be written in factorized form even when the initial and/or final states are linear combinations of $|J\Omega MvS\Lambda\Sigma\rangle$ states with J and M conserved. In the present application it will be necessary to determine expressions for the reduced matrix

elements between the various mixed states discussed in the previous section. In particular, consider the following states:

$$|JMa\rangle \equiv C|JMv_\Sigma {}^1\Sigma^+\rangle + D|JMv_\Pi {}^1\Pi_e\rangle , \tag{18a}$$

$$|J'M'a'\rangle \equiv C'|J'M'v_\Sigma {}^1\Sigma^+\rangle + D'|J'M'v_\Pi {}^1\Pi_e\rangle , \tag{18b}$$

$$|JMb\rangle \equiv |JMv_\Pi {}^1\Pi_f\rangle , \tag{18c}$$

$$|JMc\rangle \equiv F|JMv_\Sigma {}^1\Sigma^+\rangle + G|JM\bar{v}_\Pi {}^3\Pi_{0e}\rangle , \tag{18d}$$

and

$$|J'M'c'\rangle \equiv F'|J'M'v_\Sigma {}^1\Sigma^+\rangle + G'|J'M'\bar{v}_\Pi {}^3\Pi_{0e}\rangle . \tag{18e}$$

The reduced matrix elements which will be of relevance in the next section are given by the following expressions:

$$(J+1, a' || Q_1 || Ja) = C'CM_{\Sigma\Sigma}(J+1)^{1/2}$$
$$+ D'DM_{\Pi\Pi}[J(J+2)/(J+1)]^{1/2}$$
$$+ M_{\Sigma\Pi}[J^{1/2}C'D - (J+2)^{1/2}D'C] . \tag{19}$$

$$(J-1, a' || Q_1 || Ja) = -C'CM_{\Sigma\Sigma}J^{1/2}$$
$$- D'DM_{\Pi\Pi}[(J-1)(J+1)/J]^{1/2}$$
$$+ M_{\Sigma\Pi}[(J+1)^{1/2}C'D - (J-1)^{1/2}D'C] , \tag{20}$$

$$(J'a || Q_1 || Jb) = \delta(J', J)(2J+1)^{1/2}$$
$$\times \{CM_{\Sigma\Pi} + DM_{\Pi\Pi}[J(J+1)]^{-1/2}\} , \tag{21}$$

$$(J+1, c' || Q_1 || Jc) = (J+1)^{1/2}[F'FM_{\Sigma\Sigma} + G'GM_{3\Pi 3\Pi}] , \tag{22}$$

and

$$(J-1, c' || Q_1 || Jc) = -J^{1/2}[F'FM_{\Sigma\Sigma} + G'GM_{3\Pi 3\Pi}] . \tag{23}$$

Equations (19)–(23) have been obtained by use of explicit expressions for the $3j$ symbols in Eq. (16).

The quantities $M_{\Sigma\Sigma}$, $M_{\Pi\Pi}$, $M_{\Sigma\Pi}$, and $M_{3\Pi 3\Pi}$ are defined by the equations

$$M_{\Sigma\Sigma} \equiv Q_{v_\Sigma, v_\Sigma}^{1,0} , \tag{24}$$

$$M_{\Pi\Pi} = Q_{v_\Pi, v_\Pi}^{1,0} , \tag{25}$$

$$M_{3\Pi, 3\Pi} = Q_{\bar{v}_\Pi, \bar{v}_\Pi}^{1,0} , \tag{26}$$

$$M_{\Sigma\Pi} = Q_{v_\Sigma, v_\Pi}^{1,-1} . \tag{27}$$

Here, $M_{\Sigma\Sigma}$, $M_{\Pi\Pi}$, and $M_{3\Pi 3\Pi}$ are the permanent dipole moments in the Born–Oppenheimer $^1\Sigma^+$, $^1\Pi$, and $^3\Pi$ states. We shall ignore the small variation of the dipole moments with vibrational quantum number. Any errors arising from this oversight will be negligible compared to those introduced by the approximations made in our treatment of the collision dynamics (next section).

The quantity $M_{\Sigma\Pi}$ is the transition moment between the v_Σ vibrational level of the Born–Oppenheimer $^1\Sigma^+$ state and the v_Π vibrational level of the Born–Oppenheimer $^1\Pi_e$ state. It is defined explicitly by [see Eqs. (A4) and (A5)]

$$M_{\Sigma\Pi} = \langle v_\Sigma, \Lambda = 0, S = \Sigma = 0 | Q_{1-1} | v_\Pi, \Lambda = 1, S = \Sigma = 0 \rangle , \tag{28}$$

$$= \langle v_\Sigma, \Lambda = 0, S = \Sigma = 0 | Q_{11} | v_\Pi, \Lambda = -1, S = \Sigma = 0 \rangle . \tag{29}$$

This quantity is also equal to the negative of the reversed matrix element. In other words,

$$M_{\Sigma\Pi} = -M_{\Pi\Sigma} , \tag{30}$$

where

$$A_{\Pi\Sigma} = \langle v_{\Pi}, \Lambda = 1, S = \Sigma = 0 | Q_{11} | v_{\Sigma}, \Lambda = 0, S = \Sigma = 0 \rangle , \quad (31)$$

$$= \langle v_{\Pi}, \Lambda = -1, S = \Sigma = 0 | Q_{1-1} | v_{\Sigma}, \Lambda = 0, S = \Sigma = 0 \rangle . \quad (32)$$

There are no other nonvanishing matrix elements of the electric dipole operator between $^1\Pi$ and $^1\Sigma$ states. Despite the fact that the overall sign of the $^1\Sigma^+$ or $^1\Pi$ wave functions in Eqs. (28) and (29) is arbitrary, the sign of $M_{\Sigma\Pi}$ in Eqs. (19) and (20) is not. Whatever the choice of wave function sign which is made, the sign of $M_{\Sigma\Pi}$ must be consistent with the sign of the $\langle ^1\Pi | L_+ | ^1\Sigma^+ \rangle$ matrix element [Eq. (7)] which controls the relative signs of the coefficients in the mixed eigenstates [Eq. (11)]. The sign of $M_{\Sigma\Pi}$ relative to that of the $\langle ^1\Pi | L_+ | ^1\Sigma^+ \rangle$ matrix element could be determined by *ab initio* calculations.[51]

It is also possible to show that the reduced matrix elements given by Eqs. (19)–(23) satisfy the following symmetry relations:

$$(Ja || Q_1 || J \pm 1, a') = -(J \pm 1, a' || Q_1 || Ja) , \quad (33)$$

$$(Jb || Q_1 || Ja) = (Ja || Q_1 || Jb) , \quad (34)$$

and

$$(Jc || Q_1 || J \pm 1, c') = -(J \pm 1, c' || Q_1 || Jc) . \quad (35)$$

As we have discussed above, the eigenstates of the full Hamiltonian are virtually identical to the Born–Oppenheimer states, except near the isoenergetic point. Thus, the values of $M_{\Sigma\Sigma}$, $M_{\Pi\Pi}$, and $M_{3\Pi 3\Pi}$ could be taken to be the experimental dipole moments in the nominally Σ and nominally Π states, provided, of course, that the experimental measurements were not overly sensitive to the small subset of rotational levels in the region of the isoenergetic points. Alternatively, *ab initio* calculations, which naturally yield Born–Oppenheimer wave functions, could provide values for $M_{\Sigma\Sigma}$, $M_{\Pi\Pi}$, and $M_{3\Pi 3\Pi}$, as well as the for the transition moment $M_{\Sigma\Pi}$.

From Eq. (19) we see that the electronic dipole moment in a pure $^1\Sigma^+$ state, i.e., $M_{\Sigma\Sigma}$, is related to the reduced matrix element by the expression

$$M_{\Sigma\Sigma} = (-1)^{J-J'+1}(J'^1\Sigma^+ || Q_1 || J^1\Sigma^+)/(\bar{J})^{1/2} , \quad (36)$$

where $\bar{J} = \max(J, J')$. It will be convenient, when comparing the magnitude of the reduced dipole matrix elements, to avoid the square root dependency on the rotational quantum number which appears in Eqs. (19)–(23). To do so we define, consistent with Eq. (36), an effective transition dipole, given by

$$(J'\psi'_a || \mu || J\psi_a) = (-1)^{J-J'+1}(J'\psi'_a || Q_1 || J\psi_a)/(\bar{J})^{1/2} , \quad (37)$$

where ψ_a and ψ'_a will denote all the quantum numbers necessary to fully specify the state of the diatomic (Ω, v, S, Λ, Σ). Alternatively, these labels may denote linear combinations of Born–Oppenheimer states as in Eqs. (4), (5), (11), or (12).

It is instructive to use Eq. (13) to rewrite the expression for the $(J+1, a' || Q_1 || Ja)$ reduced matrix element [Eq. (19)] for the cases which are off diagonal in the electronic character of the eigenstates. Explicitly, choosing $|a\rangle = |+\rangle$ and $|a'\rangle = |-\rangle$, we find

$$(J+1, - || Q_1 || J, +) = (J+1)^{1/2} C^+_J (1 - C^{+2}_{J+1})^{1/2} M_{\Sigma\Sigma}$$

$$- [J(J+2)/(J+1)]^{1/2} C^+_{J+1}(1 - C^{+2}_J)^{1/2} M_{\Pi\Pi}$$

$$+ M_{\Sigma\Pi}\{J^{1/2}[(1 - C^{+2}_{J+1})(1 - C^{+2}_J)]^{1/2} + (J+2)^{1/2} C^+_{J+1} C^+_J\} . \quad (38)$$

Far from the isoenergetic points the $|+\rangle$ and $|-\rangle$ eigenstates are either almost entirely Σ or almost entirely Π in character. Let us assume that the $|-\rangle$ state is predominantly Π, and the $|+\rangle$ state predominantly Σ. In this case $C^+_J \simeq C^+_{J+1} \simeq 1$, so that Eq. (38) reduces to

$$(J+1, - || Q_1 || J, +) = (J+2)^{1/2} M_{\Sigma\Pi} . \quad (39)$$

Since in this limit

$$|JM + \rangle \sim |JMv_{\Sigma}{}^1\Sigma^+\rangle \quad (40)$$

and

$$|J+1, M - \rangle \sim - |J+1, Mv_{\Pi}{}^1\Pi_e\rangle , \quad (41)$$

it follows that the $(J+1, - || Q_1 || J, +)$ reduced matrix element becomes equal to the negative of the $(J+1, v_{\Pi}{}^1\Pi_e || Q_1 || Jv_{\Sigma}{}^1\Sigma^+)$ reduced matrix element, which is correct, since from Eq. (A11) the latter quantity can be shown to equal $-(J+2)^{1/2} M_{\Sigma\Pi}$. Far from the isoenergetic point, where the true eigenstates become equivalent to the Born–Oppenheimer states, the off-diagonal matrix element of the electric dipole moment is equal to the off-diagonal matrix element for the Born–Oppenheimer states. An entirely similar argument can be made in the case where the character of the $|+\rangle$ and $|-\rangle$ states is reversed.

Near the isoenergetic point, where the mixing of the two Born–Oppenheimer states is substantial, both the C^+_J and C^+_{J+1} coefficients will be substantially reduced from unity, so that the first two terms in Eq. (38) will make a contribution to the reduced matrix elements. In the hypothetical limit where $C^+_J \simeq C^+_{J+1} \simeq 2^{-1/2}$, we find

$$(J+1, - || Q_1 || J, +) = (1/2)\{(J+1)^{1/2} M_{\Sigma\Sigma}$$

$$- [J(J+2)/(J+1)]^{1/2} M_{\Pi\Pi}\}$$

$$+ (1/2)[J^{1/2} + (J+2)^{1/2}] M_{\Sigma\Pi} . \quad (42)$$

At moderate to large values of J, this can be approximated very accurately by

$$(J+1, - || Q_1 || J, +) \simeq (J+1)^{1/2}[(1/2)(M_{\Sigma\Sigma} - M_{\Pi\Pi}) + M_{\Sigma\Pi}] . \quad (43)$$

Thus, the off-diagonal matrix element of the electric dipole operator becomes enhanced from its value far from the isoenergetic point [Eq. (39)]. In practice, due to the minus sign in Eq. (38), it is also possible for coincidental zeros of the reduced matrix element to occur. If we neglect the value of $M_{\Sigma\Pi}$, we see that a zero will occur for

$$\frac{M_{\Sigma\Sigma}}{M_{\Pi\Pi}} = \frac{C^+_{J+1}[J(J+2)(1 - C^{+}_J)]^{1/2}}{(J+1)C^+_J(1 - C^{+2}_{J+1})^{1/2}} \simeq \frac{C^+_{J+1}(1 - C^{+2}_J)^{1/2}}{C^+_J(1 - C^{+2}_{J+1})^{1/2}} . \quad (44)$$

A similar analysis can be applied to the states arising from the mixing of the $^1\Sigma^+$ and $^3\Pi_{0e}$ levels [Eq. (12)]. Again, far from the isoenergetic point, we shall assume that the $|JM +\rangle$ state is predominantly $^1\Sigma^+$, so that $F^+_J \simeq F^+_{J+1} \simeq 1$ [Eq. (12)], and that the $|J+1, M -\rangle$ state is predominantly $^3\Pi_{0e}$, i.e.,

$$|J+1, M-\rangle \simeq -|J+1, Mv_\Pi{}^3\Pi_{0e}\rangle . \tag{45}$$

In this limit it is easy to show that the off-diagonal reduced matrix element [Eq. (22)] becomes

$$(J+1, -||Q_1||J, +) \simeq 0 , \tag{46}$$

which is to be expected, since in the Born–Oppenheimer limit there is no dipole coupling between a $^3\Pi$ and a $^1\Sigma^+$ state. Near the isoelectronic point, the limiting behavior of the reduced matrix elements can be obtained in a manner similar to that described in the preceding paragraphs. We find

$$(J+1, -||Q_1||J+) \simeq \tfrac{1}{2}(J+1)^{1/2}(M_{\Sigma\Sigma} - M_{3\Pi^3\Pi}) . \tag{47}$$

Thus, even if the actual value of the Born–Oppenheimer Σ–Π transition moment is small or vanishing (as in the case of $^1\Sigma^+$–$^3\Pi$), there can exist, in the region of the largest non-Born–Oppenheimer mixing, substantial transition moments between the eigenstates of the full Hamiltonian. This is particularly true if there is a substantial difference between the permanent dipole moments in the Σ and Π states. Cross sections for collisional energy transfer are proportional to the squares of the reduced dipole matrix elements, as will be discussed in the next section.

IV. COLLISION DYNAMICS

As discussed in the Introduction, our treatment of the collision dynamics is similar to that of Chiu,[29] except that the time-dependent rather than time-independent Born approximation is used. The formalism presented below represents an extension, to collisions between molecular states of nonzero angular momentum, of methods used by Gray and van Kranendonk,[34] Rabitz,[35] and Sharma and Brau.[36]

The interaction potential between two diatomic molecules is expanded in the standard multipolar series[29,52]

$$V = \sum_{l_a l_b} (-1)^{l_b}[(2l)!/(2l_a)!(2l_b)!]^{1/2} T_l(\mathbf{r}_a\mathbf{r}_b) \cdot U_l(\mathbf{R}) . \tag{48}$$

Here $l = l_a + l_b$, $\mathbf{r}_a$ and $\mathbf{r}_b$ denote, collectively, the coordinates of all the electrons and nuclei in molecules a and b, respectively, $\mathbf{R}$ is the vector joining the centers of mass of the two molecules, and the quantity $U_l(\mathbf{R})$ is a spherical tensor[49] with components

$$U_{lm}(\mathbf{R}) = [4\pi/(2l+1)]^{1/2} R^{-l-1} Y_{lm}(\mathbf{R}) . \tag{49}$$

Also, the quantity $T_l(\mathbf{r}_a\mathbf{r}_b)$ denotes a tensor product of two spherical tensors with components

$$T_{lm}(\mathbf{r}_a\mathbf{r}_b) = \sum_{m_a m_b} (l_a m_a l_b m_b | l_a l_b lm) Q_{l_a m_a}(\mathbf{r}_a) Q_{l_b m_b}(\mathbf{r}_b) , \tag{50}$$

where $(lml'm'|ll'l''m'')$ is a Clebsch–Gordan coefficient and the spherical tensor operator $Q_{lm}(\mathbf{r})$ is the operator for the lth electric multipole, defined, in generalization of Eq. (14), as[48]

$$Q_{lm}(\mathbf{r}) = e[4\pi/(2l+1)]^{1/2} \sum_i r_i^l Y_{lm}(\hat{r}_i) . \tag{51}$$

We further recall that the scalar product of two tensor operators is given by the expression[49]

$$T_l \cdot U_l = \sum_m (-1)^m T_{lm} U_{l-m} . \tag{52}$$

In the time-dependent first Born approximation, the amplitude for a transition between an initial state $|i\rangle$ and a final state $|f\rangle$ is given by[34-37]

$$A_{if}(b) = \hbar^{-1} \int_{-\infty}^{+\infty} \exp(i\omega_{if}t) \langle f| V(t;b) |i\rangle \, dt , \tag{53}$$

where ω_{if} is equal to the inelastic energy gap divided by $\hbar$, and $V(t;b)$ is the time-dependent interaction potential obtained from Eq. (48) by assumption of a time-dependent trajectory $\mathbf{R} = \mathbf{R}(t;b)$, where b is the impact parameter. The initial and final states are products of eigenstates of the Hamiltonian for the isolated molecules, which will, of course, include the non-Born–Oppenheimer coupling within each molecule. In other words,

$$|i\rangle = |J_a M_a \psi_a\rangle |J_b M_b \psi_b\rangle \tag{54}$$

and

$$|f\rangle = |J_a' M_a' \psi_a'\rangle |J_b' M_b' \psi_b'\rangle , \tag{55}$$

where ψ_a, ψ_a', ψ_b, and ψ_b' are composite indices as defined in the preceding section.

The matrix elements of the electric multipole operators $Q_{l_a m_a}(\mathbf{r}_a)$ and $Q_{l_b m_b}(\mathbf{r}_b)$ can be written in factorized form; explicit expressions are given in the Appendix. Thus, it is possible to express the transition amplitude as

$$A_{if}(b) = \hbar^{-1} \sum_{l_a l_b} (-1)^{l_b}[(2l)!/(2l_a)!(2l_b)!]^{1/2}(-1)^{J_a'+J_b'-M_a'-M_b'}$$

$$(J_a'\psi_a'||Q_{l_a}||J_a\psi_a)(J_b'\psi_b'||Q_{l_b}||J_b\psi_b) \sum_{\substack{m_a m_b \\ m}} (l_a m_a l_b m_b | l_a l_b lm)(-1)^m \begin{pmatrix} J_a' & l_b & J_a \\ -M_a' & m_a & M_a \end{pmatrix} \begin{pmatrix} J_b' & l_b & J_b \\ -M_b' & m_b & M_b \end{pmatrix} I_m^l(\omega_{if}, b) , \tag{56}$$

where

$$I_m^l(\omega_{if}, b) = \int_{-\infty}^{+\infty} U_{l-m}[\mathbf{R}(t;b)] \exp(i\omega_{if}t) \, dt . \tag{57}$$

It is convenient following Gray and van Kranendonk[34] to define the dimensionless variables

$$z = vt/b , \tag{58}$$

$$x_{if} = \omega_{if} b/v , \tag{59}$$

$$\rho(z;b) = R(bz/v;b)/b . \tag{60}$$

n terms of these, the integral I_m^l can be written as

$$I_m^l(\omega_{if}, b) = (1/vb^{2l})J_m^l(\omega_{if}, b) ,$$

(61)

where $J_m^l(\omega_{if}, b)$ is dimensionless and given by

$$J_m^l(\omega_{if}, b) = \int_{-\infty}^{+\infty} U_{l-m}[\rho(z;b)] \exp(ixz) dz .$$

(62)

The unpolarized transition probability is defined by

$$P_{J_a\psi_a J_b\psi_b \to J_a'\psi_a' J_b'\psi_b'} = [(2J_a+1)(2J_b+1)]^{-1} \sum_{\substack{M_a M_a' \\ M_b M_b'}} |A_{J_aM_a\psi_a J_bM_b\psi_b \to J_a'M_a'\psi_a' J_b'M_b'\psi_b'}|^2 .$$

(63)

When expression (56) is squared and the sums over M_a, M_a', M_b, M_b', m_a, and m_b are carried out, considerable simplification occurs from the orthogonality relations involving the $3j$ symbols and Clebsch–Gordan coefficients. The result is

$$P_{J_a\psi_a J_b\psi_b \to J_a'\psi_a' J_b'\psi_b'}(b) = \sum_{l_a l_b} \frac{(2l)!(J_a'\psi_a'||Q_{l_a}||J_a\psi_a)^2 (J_b'\psi_b'||Q_{l_b}||J_b\psi_b)^2}{(2l_a+1)!(2l_b+1)!(2J_a+1)(2J_b+1)\hbar^2 b^{2l}v^2} \sum_{m=-l}^{l} |J_m(\omega_{if}, b)|^2 .$$

(64)

For the case of transitions between states which are linear combinations of the Hund's case (a) states, the reduced matrix elements are linear combinations of the Hund's case (a) reduced matrix elements, as exemplified in the discussion in the preceding section.

If the relative motion of the two collision partners is treated as rectilinear, then the J_m^l integrals can be evaluated to yield[34]

$$\sum_m |J_m^l(\omega_{if}, b)|^2 = 4x_{if}^{2l} \sum_m \frac{[K_m(x_{if})]^2}{(l-m)!(l+m)!} ,$$

(65)

where x_{if} is defined by Eq. (59) and $K_m(x)$ is a modified Bessel function. In an actual application Eq. (65) can be well approximated as[36,53]

$$\sum_m |J_m^l(\omega_{if}, b)|^2 = 4 \exp(-2x_{if})(A_l + B_l x_{if} + C_l x_{if}^2 + \cdots) ,$$

(66)

where values of the coefficients have been presented by Cross and Gordon[53] as well as by Sharma and Brau.[36]

For dipole–dipole collisions $(l_a = l_b = 1)$ between molecules in $^1\Sigma^+$ electronic states, the square of the reduced matrix elements have the simple form

$$(J_a'v_C\,^1\Sigma^+||Q_1||J_av_C\,^1\Sigma^+)^2 = M_{CC}^2(2J_a+1)(J_a010|J_a1J_a'0)^2 ,$$

(67)

where M_{CC} is the permanent dipole moment. In this case Eq. (64) reduces to expressions which have been given previously.[34-36]

The integral cross section is obtained by integration over the impact parameter

$$\sigma_{J_aJ_b \to J_a'J_b'} = 2\pi \int_0^\infty bP_{J_aJ_b \to J_a'J_b'}(b) db ,$$

(68)

where for simplicity the ψ_a, ψ_a', ψ_b', and ψ_b indices have been surpressed. The first Born transition probability increases monotonically as the impact parameter is decreased and in the usual application this increase is artificially halted by setting the transition probability equal to a constant value for impact parameters less than the value for which $P(b)$ exceeds a physically reasonable limit. As we have discussed before,[38,54] within the cutoff region the truncated transition probability no longer satisfies statistical microreversibility, which requires

$$(2J_a+1)(2J_b+1)P_{J_aJ_b \to J_a'J_b'} = (2J_a'+1)(2J_b'+1)P_{J_a'J_b' \to J_aJ_b} .$$

(69)

It is possible to correct for this by the simple redefinition of the transition probability as

$$P_{J_aJ_b \to J_a'J_b'} = [J_a'^{>}J_b'^{>}/(2J_a+1)(2J_b+1)]P^0_{J_aJ_b \to J_a'J_b'} ,$$

(70)

where

$$P^0_{J_aJ_b \to J_a'J_b'} = \frac{(2l)!(J_a'\psi_a'||Q_{l_a}||J_a\psi_a)^2 (J_b'\psi_b'||Q_{l_b}||J_b\psi_b)^2}{(2l_a+1)!(2l_b+1)! J_a'^{>}J_b'^{>}}$$
$$\times \sum_{m=-l}^{+l} |J_m^l(\omega_{if}, b)|^2 .$$

(71)

Then the cutoff procedure can be defined as follows:

$$\sigma_{J_aJ_b \to J_a'J_b'} = \pi[J_a'^{>}J_b'^{>}/(2J_a+1)(2J_b+1)]$$
$$\times \left[b_c^2 P_c + 2\int_{b_c}^\infty b P^0_{J_aJ_b \to J_a'J_b'}(b) db \right] ,$$

(72)

where the cutoff impact parameter b_c is chosen so that

$$P^0_{J_aJ_b \to J_a'J_b'}(b = b_c) = P_c .$$

(73)

In the specific case of dipole–dipole scattering between two molecules in a $^1\Sigma^+$ state the reduced dipole matrix elements are given by Eq. (67). Since

$$(J_a010|J_a1J_a'0)^2 = J_a^{>}/(2J_a+1) ,$$

(74)

it can be easily shown that the microreversible Born approximation defined by Eqs. (70)–(73) reduces identically in this case to the definition made in our earlier work.[38]

In a previous study[38] of rotationally inelastic LiH($j=1$) + HCN collisions, where P_c was given the conventional value of unity, we found that the integral cross sections predicted by the microreversible Born approximation were approximately twice as large as the values predicted by the presumably more accurate adiabatically corrected sudden approximation,[38,55,56] which we have recently developed. Accordingly, in the present study we impose a cutoff value of

$$P_c = 0.5 .$$

(75)

TABLE I. Parameters describing Born–Oppenheimer $A\,^1\Sigma^+$, $a\,^3\Pi_0$, and $A'\,^1\Pi$ states in CaO.

Parameter	$A\,^1\Sigma^+$	$A'\,^1\Pi$	$a\,^3\Pi_0$
$\omega_e\,^a$	718.9	557.5	556.2
$\omega_e x_e\,^a$	−2.11	−3.31	−3.3
$B_e\,^a$	0.4059	0.3353	0.3353
$\alpha_e\,^a$	0.00137	0.0015	0.0015
$\nu_{00}\,^b$	0.0	−2985	−3165
M^c	8.72	3.32	3.41

^{a}From Ref. 21.

^{b}Band origin of the $v=0$, $J=0$ level, measured with respect to the $v=0$, $J=0$ level of the $A\,^1\Sigma^+$ state. The value for the $A'\,^1\Pi$ state is taken from Ref. 21. The value for the $a\,^3\Pi_0$ state is adjusted so that the lowest isoenergetic point $(v_\Sigma=0,\ v_\Pi=7)$ will occur at a rotational quantum number of $J=74.6$, the experimentally observed value (Ref. 21).

^{c}Electronic dipole moment, in D, from Ref. 59. The entries correspond, from left to right, to the quantities $M_{\Sigma\Sigma}$ [Eq. (24)], $M_{\Pi\Pi}$ [Eq. (25)], and $M_{3\Pi\,3\Pi}$ [Eq. (26)].

We expect that the microreversible Born approximation, described above, will provide a reasonable description of the collisional energy transfer within and between the rotational manifolds resulting from non-Born–Oppenheimer mixing of the $A\,^1\Sigma^+$ and neighboring Π states. A discussion of the potential sources of error in our treatment of the dynamics is deferred until Sec. VII of this paper.

V. CROSS SECTIONS AND RATE CONSTANTS FOR COLLISIONS BETWEEN CaO* and N₂O

In this section we apply the formalism described in the preceding section to the calculation of cross sections and rate constants for energy transfer in collisions of CaO with N_2O. We shall assume pure dipole-dipole coupling and consider collisions between the various CaO states arising from the orbit–rotation mixing of the $v_\Sigma=0$, $v_\Pi=4–11$ and $v_\Sigma=1$, $v_\Pi=7–11$ levels of the Born–Oppenheimer states which have the spectroscopic designation $A\,^1\Sigma^+$ and $A'\,^1\Pi_e$; and between the various CaO states arising from the spin–orbit mixing of the $v_\Sigma=0$, $v_\Pi=6–16$ and $v_\Sigma=1$, $v_\Pi=8–12$ levels of the Born–Oppenheimer states which have the spectroscopic designation $A\,^1\Sigma^+$ and $a\,^3\Pi_{0e}$. As stated in Sec. II, $^1\Sigma^+ - ^1\Pi_e$ and $^1\Sigma^+ - ^3\Pi_{0e}$ mixings are considered separately. Also, we will explicitly investigate collisional transfer between the $^1\Pi_f$ and $^1\Pi_e$ rotational levels in the $v_\Pi=6$ level of the Born–Oppenheimer $^1\Pi$ state. The $^1\Pi_f$ and $^1\Pi_e$ levels are split by the mixing which occurs between the latter and the $v_\Sigma=0$ level of the $A\,^1\Sigma^+$ state.

The details of the non-Born–Oppenheimer mixing were treated as follows: RKR curves for the Born–Oppenheimer $A\,^1\Sigma^+$, $A'\,^1\Pi$, and $a\,^3\Pi_0$ states were calculated using the spectroscopic constants given by Field,[21] which are listed in Table I. The orbit–rotation and spin–orbit matrix elements [Eqs. (6) and (8)] were obtained using the values of $\langle v_\Pi|B|v_\Sigma\rangle$ and $\langle v_\Pi|v_\Sigma\rangle$ computed from the vibrational wave functions from Numerov integration of the RKR curves and using the experimental strength constants given by Field ($b=1.30$, $a_+=110$ cm^{-1}). The values of these matrix elements are listed in Table II.

In the calculation of the inelastic cross sections the target was assumed to be N_2O in the $\bar{X}\,^1\Sigma^+$ state with dipole moment of $M_b=0.167$ D[57] and rotational constant of $B=0.4182$ cm^{-1}.[58] For CaO, the permanent moments $M_{\Sigma\Sigma}$, $M_{\Pi\Pi}$, and $M_{3\Pi3\Pi}$ were taken from the ab initio calculation of England[59] and are listed in Table I. Due to the strongly polar character of CaO, these three permanent moments are presumably of the same sign. Nothing is known about the transition moment $M_{\Sigma\Pi}$ [Eq. (27)]. In the simplest one electron description of the excited states of CaO, the A and A' states have the electronic configurations[60]

TABLE II. Strength of non-Born–Oppenheimer coupling between $A\,^1\Sigma^+$ and $A'\,^1\Pi_e$ or $a\,^3\Pi_{0e}$ states in CaO.

	$v_\Sigma=0$		$v_\Sigma=1$	
v_Π	Orbit–rotation^a	Spin–orbit^b	Orbit–rotation^a	Spin–orbit^b
3	0.310			
4	0.319			
5	0.297			
6	0.256	18.3		
7	0.206	14.6	0.267	
8	0.156	11.0	0.271	18.8
9	0.111	7.79	0.244	16.9
10	0.0753	5.27	0.201	13.8
11	0.0482	3.39	0.152	10.5
12		2.06		7.50
13				5.01

^{a}Values of orbit–rotation coupling in cm^{-1}, defined as [Eq. (6)] $|\,2^{1/2}\,b\,\langle v_\Pi|B|v_\Sigma\rangle\,|$, where $b=1.30$ cm^{-1} (Ref. 21). The complete perturbation matrix element is then obtained by multiplication by $[J(J+1)]^{1/2}$.

^{b}Values of spin–orbit coupling in cm^{-1}, defined as [Eq. (8)] $|\,\frac{1}{2}\,a_+\langle v_\Pi|v_\Sigma\rangle\,|$, where $a_+=110$ cm^{-1} (Ref. 21).

$$A\,^1\Sigma^+ = \cdots\, 8\sigma9\sigma3\pi^4 \tag{76}$$

.nd

$$A'\,^1\Pi = \cdots\, 8\sigma^29\sigma3\pi^3 \ . \tag{77}$$

Analysis of the normalized Mulliken populations reported by Bauschlicher and Yarkony[60] shows that both the 8σ and 3π orbitals are highly localized on the O atom and correspond, respectively, to the O $2p_\sigma$ and $2p_r$ atomic orbitals.

Since the electric dipole operator is a one-electron operator and since the MO descriptions of the $A\,^1\Sigma^+$ and $A'\,^1\Pi$ states differ in the occupation of the 8σ and 3π orbitals, the electronic expectation value will be given by just the expectation value of the one-electron dipole operator taken between these two orbitals,[61] so that the value of $M_{\Sigma\Pi}$ can be shown to be [from Eq. (A6)]

$$M_{\Sigma\Pi} \simeq \langle v_\Sigma | v_\Pi \rangle e (4\pi/3)^{1/2} \int 3\pi^*_{-1}(\mathbf{r}) r Y_{1\text{-}1}(\mathbf{r}) 8\sigma(\mathbf{r})\, d\mathbf{r} \ . \tag{78}$$

The integral will be very small, since the 3π and 8σ orbitals are basically $2p_r$ and $2p_\sigma$ atomic orbitals between which the transition dipole is identically zero. Any residual value will be further reduced by the vibrational overlap, which is ~ 0.05–0.1 for the Σ–Π mixings under consideration here. Accordingly, in the absence of *ab initio* calculations to determine the precise value of the electronic integral in Eq. (78) we shall make the reasonable assumption that

$$M_{\Sigma\Pi} \simeq 0 \ . \tag{79}$$

This choice eliminates, of course, the necessity of determining the relative signs of $M_{\Sigma\Pi}$ and the $\langle\,^1\Pi | L_+ | \,^1\Sigma^+ \rangle$ matrix element [Eq. (7)].

The reduced matrix elements which appear in the expression for the cross sections [Eq. (71)] are given by Eqs. (19)–(23) for the CaO molecule. It is important to observe that because $M_{\Sigma\Pi}$ is taken to be zero, the reduced dipole matrix element for the coupling between the $\,^1\Pi_f$ levels and the levels which are nominally $\,^1\Pi_e$ is given by [Eq. (21)]

$$(J_a\psi'_a | | Q_1 | | J_a\psi_a) = DM_{\Pi\Pi}[(2J+1)/J(J+1)]^{1/2} \ . \tag{80}$$

The square of this matrix element will decrease linearly with J_a, in contrast with the other reduced matrix elements [Eqs. (19), (20), (22), and (23)] whose squares *increase* linearly with J_a. Thus, we expect the $\,^1\Pi_f$–$\,^1\Pi_e$ collisional coupling to be unimportant except at low values of J. Rabitz[35] has made a similar observation in connection with his study of dipolar energy transfer between l-doubled levels of symmetric top molecules.

The reduced dipole matrix element for the N_2O molecule, which is in a $\,^1\Sigma^+$ electronic state, is given by Eq. (67), with the a index replaced everywhere by b.

Thermal rate constants can be determined from the integral cross sections [Eq. (72)] by summing and averaging over the N_2O rotational states and by integrating over an assumed Maxwellian distribution of relative $(CaO\text{–}N_2O)$ collision velocities, in other words[62]

$$k_{J_a\psi_a\to J'_a\psi'_a}(T_{\text{tr}}) = \left[\frac{8}{\pi m(kT_{\text{tr}})^3}\right]^{1/2}$$
$$\times \int_0^\infty \sigma_{J_a\psi_a\to J'_a\psi'_a}(E) E \exp(-E/kT_{\text{tr}})\, dE \ , \tag{81}$$

where m is the collision reduced mass and T_{tr} is the assumed translational temperature. The cross section which appears in the integrand of Eq. (81) is obtained from the degeneracy averaged integral cross section of Eq. (72) by summing and averaging over the rotational states of the target molecule (N_2O) in electronic state b. We have

$$\sigma_{J_a\psi_a\to J'_a\psi'_a} = z_b^{-1}(T_r) \sum_{J_b J'_b} (2J_b + 1)$$

$$\times \exp[-B_b J_b(J_b+1)/kT_r]\sigma_{J_a\psi_a J_b\psi_b\to J'_a\psi'_a J'_b\psi'_b} , \tag{82}$$

where z_b denotes the rotational partition function of the target with rotational temperature T_r and rotational constant B_b. Note that the ψ_b index is unchanged since the N_2O molecule is assumed to remain in its ground electronic state.

In the calculations to be reported here the N_2O rotational temperature was taken to be 300 K and the translational temperature [Eq. (81)] was 4800 K. The latter value corresponds to a most probable relative velocity of 1.8×10^5 cm/s, a value which seems appropriate to the experiments of Irvin and Dagdigian.[7] The integral over the relative translational energy in Eq. (81) was evaluated numerically, which necessitates at each quadrature energy the calculation of a complete set of microreversible Born cross sections. We found that adequate accuracy could be achieved with three-point Gauss–Legendre quadrature.

VI. RESULTS

Figure 2 displays the dependence of the rotational quantum number of the effective transition dipole matrix element $(J\psi'_a | | \mu | | J+1, \psi_a)$ [Eq. (37)] for transitions in which the ψ'_a state is nominally $\,^1\Pi_e$ and the ψ_a state is nominally $\,^1\Sigma^+$. The matrix elements are displayed for the non-Born–Oppenheimer mixing between the $v_\Sigma = 0$ and $v_\Pi = 6$, 8, and 10 levels. Since the $|+\rangle$ and $|-\rangle$ states change their predominant character at the isoenergetic point, for the $J \to J+1$ transition which straddles the value of J_{cross} [Eq. (10)] the (nominally) $\,^1\Pi_e \to\,^1\Sigma^+$ transition corresponds to the $|+\rangle \to |+\rangle$ transition. In this case the reduced matrix can be shown, in analogy with the development leading to Eq. (43)

$$(J+ | | \mu | | J+1, +) \simeq (1/2)(M_{\Sigma\Sigma} + M_{\Pi\Pi}) = 6.0 \text{ D} \ ,$$

which obviously is considerably larger than the values near, but not right at, the isoenergetic point, given roughly by Eq. (43). The transition dipoles are seen to be substantial over a wide range of rotational levels surrounding the isoenergetic point. The width of the transition dipole distribution decreases at the higher isoenergetic points because the rotational energy spacings are larger at larger values of J, so that only the levels nearest the isoenergetic point become effectively mixed. Since the cross sections for energy
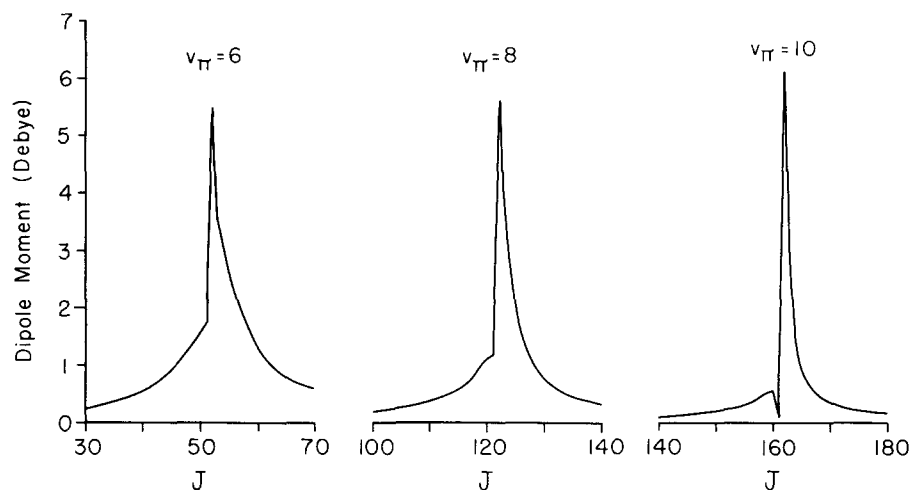
FIG. 2. Dependence on the rotational quantum number of the effective dipole matrix element $(J \psi_a' \| \mu \| J+1, \psi_a)$ [Eq. (37)] for transitions in which the ψ_a' state is nominally $^1\Pi_e$, $v_\Pi = 6$, 8, or 10 and in which the ψ_a state is nominally, $^1\Sigma^+$, $v_\Sigma = 0$. The dip in the value of the $v_\Pi = 10$ dipole matrix element above $J = 160$ corresponds to the type of accidental cancellation discussed in Sec. IV and illustrated by Eq. (44).

transfer are proportional to the square of the reduced dipole matrix element [Eq. (71)], we expect that significant $^1\Pi_e \rightarrow {}^1\Sigma^+$ population transfer will take place over a similarly broad range of rotational levels.

Figure 3 displays the calculated energies of the $^1\Sigma^+$, $v_\Sigma = 0$ and $^1\Pi_e$, $v_\Pi = 6$ rotational ladders in the region of the isoenergetic point, where the mixing between the Born–Oppenheimer states is the strongest. Also indicated are the microreversible Born cross sections for collision induced transitions between these levels, calculated at a collision velocity of 1.8×10^5 cm/s, which corresponds to the most probable value in the assumed distribution of relative translational velocities. Transitions between levels which are labeled A or which are labeled A', i.e., between mixed states which are either predominately A or A' in character, correspond to pure rotational relaxation. As can be seen from Fig. 2, the cross sections for these processes are very large. Addition of the cross sections for the downward transitions, which could be obtained from those shown in Fig. 2 by applying statistical microreversibility, would lead to total cross sections of ~ 120 Å^2 for rotational relaxation. Recently, Gottscho, Field, Bacis, and Silvers have described[63] an optical–optical double resonance study of rotational energy transfer in BaO($A^1\Sigma^+$) with CO_2 as a collision partner. They report total inelastic cross sections ranging from 50 ± 20 to 230 ± 40 Å^2, depending on the initial rotational level. These values are certainly consistent with our calculated value of ~ 120 Å^2.

Figure 4 displays rate constants for $J \rightarrow J+1$ transfer within the (nominally) $v_\Sigma = 0$ level of the $A^1\Sigma^+$ state as well as rate constants for transfer into the (nominally) $v_\Sigma = 0$, $A^1\Sigma^+$ state from successively higher vibrational levels of the (nominally) $A'^1\Pi_e$ state. Each maximum corresponds to transfer occurring from a successively higher vibrational level of the A' state (see Fig. 1). Far from the isoenergetic points the (nominally) $A \rightarrow$ (nominally) A transfer corresponds to pure rotational relaxation within the $A^1\Sigma^+$ state. The rates drop slightly with increasing rotational quantum number due to the increasing energy gap between successive rotational levels. The rate constants for (nominally) $A'^1\Pi_e \rightarrow$ nominally $A^1\Sigma^+$ energy transfer are smaller, except right at the

isoenergetic points, where the predominant electronic character of the mixed states becomes so confused. Because experimental studies indicate that nascent alkaline earth oxide molecules can be formed with a large degree of rotational excitation, it is important
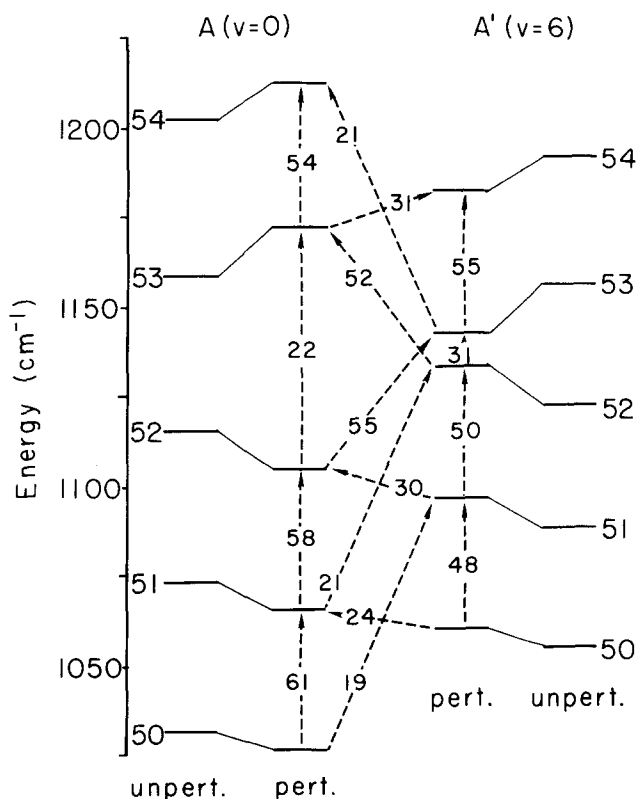

FIG. 3. Rotational energy levels in the $A^1\Sigma^+$ $(v = 0)$ and $A'^1\Pi$ $(v = 6)$ manifolds of CaO in the vicinity of the isoenergetic point. The zero of energy refers to the $v = 0$, $J = 0$ level of the $A^1\Sigma^+$ state. The position of the levels is shown both with and without inclusion of the orbit–rotation perturbation. The various levels are denoted A or A' depending on their predominant character. Also indicated are microreversible Born cross sections for all the dipole allowed upward transitions induced by collisions with N_2O, calculated using an assumed translational velocity of 1.8×10^5 cm/s, and averaged over a 300 K Boltzmann distribution of N_2O rotational levels.

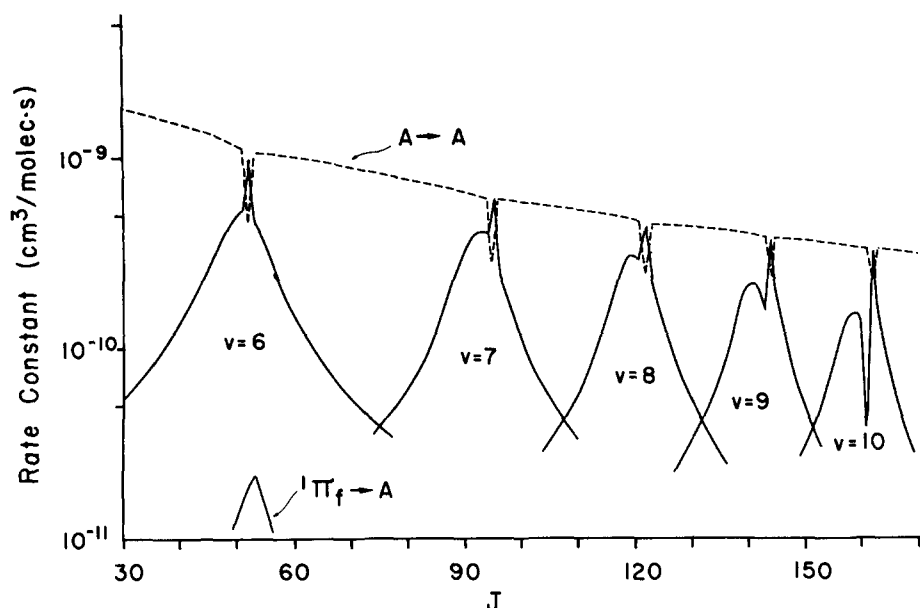FIG. 4. Rate constants for upward $(J \to J+1)$ collisional energy transfer within the $v_\Sigma = 0$ rotational manifold of the (nominally) $A\,^1\Sigma^+$ state as well as for transfer into the $v_\Sigma = 0$ manifold from successively higher vibrational levels of the (nominally) $A'\,^1\Pi_e$ state. The successive maxima correspond to the occurrence of successive isoenergetic points (Fig. 1). For clarity the rates have been drawn as continuous curves although they are defined only for integer values of J. Also shown are rates for Q-branch $(J \to J)$ transfer into the $v_\Sigma = 0$, $A\,^1\Sigma^+$ state from the $v_\Pi = 6$ manifold of the $A'^1\Pi_f$ Λ-doubled component. This transfer occurs only because of non-Born–Oppenheimer mixing between the $A\,^1\Sigma^+$ and $A'\,^1\Pi_e$ states.

to consider electronic transfer even at very high values of the rotational quantum number. We note in Fig. 4 that the width of the region of substantial transfer becomes successively narrower at the higher isoenergetic points because, as discussed earlier in this section, the larger rotational level spacings act to limit the significant region of non-Born–Oppenheimer mixing.

The orbit–rotation perturbation matrix element [Eq. (6)] increases linearly with the rotational quantum number. Thus, for this reason one might expect that at very high values of J the mixing between the Born–Oppenheimer levels will be large despite the lack of energy resonance. If this is true, then substantial transition

dipole moments will occur and the cross sections for $^1\Pi_e \to {}^1\Sigma^+$ energy transfer will be large and virtually independent of J. Indeed, this type of mechanism has been suggested in BaO.[20] To investigate this possibility we have calculated the rate constants for transfer into the (nominally) $v_\Sigma = 0$ level of the $A\,^1\Sigma^+$ state from high rotational levels $(J > 100)$ of the $v_\Pi = 4$, 5, and 6 manifolds of the $A'\,^1\Pi_e$ state. The calculated rate constants were found to be less than 1×10^{-11} cm^3/molecule s, in other words negligibly small compared to the other transfer rate constants displayed in Fig. 4.

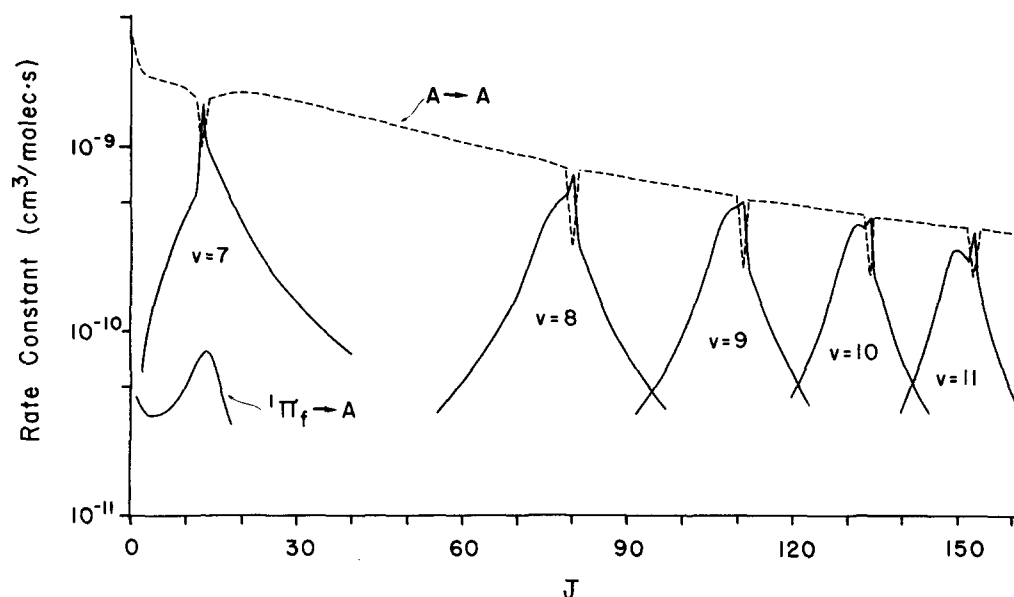In Fig. 5 we present similar rates for collisional transfer into the (nominally) $v_\Sigma = 1$ level of the $A\,^1\Sigma^+$

FIG. 5. Rate constants for upward $(J \to J+1)$ collisional energy transfer within the $v_\Sigma = 1$ rotational manifold of the (nominally) $A\,^1\Sigma^+$ state as well as for transfer into the $v_\Sigma = 1$ manifold from successively higher vibrational levels of the (nominally) $A'^1\Pi_e$ state. The successive maxima correspond to the occurence of successive isoenergetic points (Fig. 1). For clarity the rates have been drawn as continuous curves although they are defined only for integer values of J. Also shown are rates for Q-branch $(J \to J)$ transfer into the $v_\Sigma = 1$, $A\,^1\Sigma^+$ state from the $v_\Pi = 7$ manifold of the $A'\,^1\Pi_f$ Λ-doubled component. This transfer occurs only because of non-Born–Oppenheimer mixing between the $A\,^1\Sigma^+$ and $A'\,^1\Pi_e$ states.
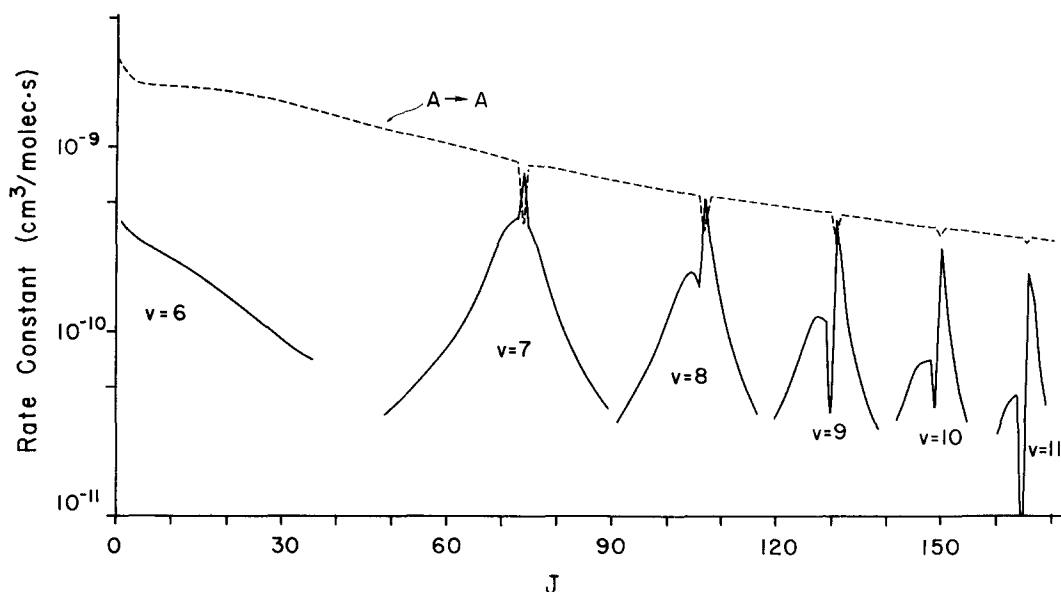
FIG. 6. Rate constants for upward $(J \to J+1)$ collisional energy transfer within the $v_\Sigma = 0$ rotational manifold of the (nominally) $A\,^1\Sigma^+$ state as well as for transfer into the $v_\Sigma = 0$ manifold from successively higher vibrational levels of the (nominally) $a\,^3\Pi_{0e}$ state. The successive maxima correspond to the occurrence of successive isoenergetic points. For clarity the rates have been drawn as continuous curves although they are defined only for integer values of J.

state from successively higher vibrational levels of the (nominally) $A'\,^1\Pi_e$ state from successively higher vibrational levels of the (nominally) $A'\,^1\Pi_e$ state. The graph is qualitatively identical to Fig. 4, except that the first isoenergetic point occurs at a lower value of J. We observe here as in Fig. 4 a sharp minimum in the transfer rates very near some of the higher isoenergetic points. This arises from the accidental cancellation of the $\Pi_e \to \Sigma$ reduced dipole matrix element which has been discussed previously (Sec. III) and which can be seen in Fig. 2.

Figures 6 and 7 present rates for collisional transfer into the (nominally) $v_\Sigma = 0$ and 1 levels of the $A\,^1\Sigma^+$ state from successively higher vibrational levels of the (nom-

inally) $a\,^3\Pi_{0e}$ state. We observe the same qualitative features as seen in Figs. 4 and 5. The rise in the energy transfer rate at low J in Fig. 6 corresponds to transfer from the $v_\Pi = 6$ level of the $^3\Pi_{0e}$ state. In this case there is no actual isoenergetic point; it would lie at a complex value of the total angular momentum.

A comparison with experimental results on other systems is worthwhile. In a study of energy transfer between the $X\,^2\Sigma^+$ and $A\,^2\Pi$ states of CN, Katayama, Miller, and Bondybey[26] found that with Ar as a collision partner the rate constants for transfer between the energetically nearest vibrational levels ranged from 3×10^{-11} to $\sim 2 \times 10^{-10}$ cm^3/molecule s. These values are somewhat less than the calculated values for the CaO* + N$_2$O system
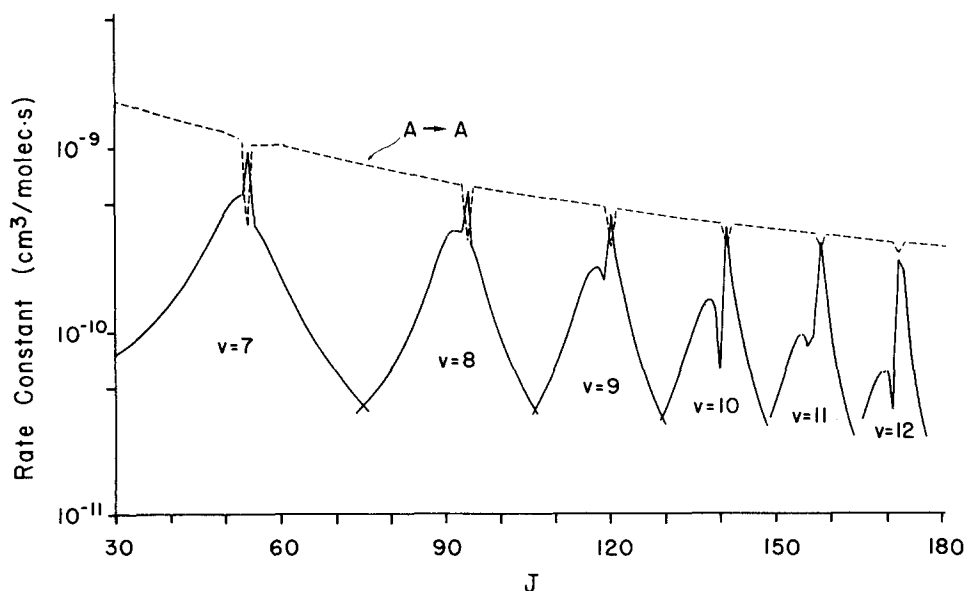

FIG. 7. Rate constants for upward $(J \to J+1)$ collisional energy transfer within the $v_\Sigma = 1$ rotational manifold of the (nominally) $A\,^1\Sigma^+$ state as well as for transfer into the $v_\Sigma = 1$ manifold from successively higher vibrational levels of the (nominally) $a\,^3\Pi_{0e}$ state. The successive maxima correspond to the occurrence of successive isoenergetic points. For clarity the rates have been drawn as continuous curves although they are defined only for integer values of J.
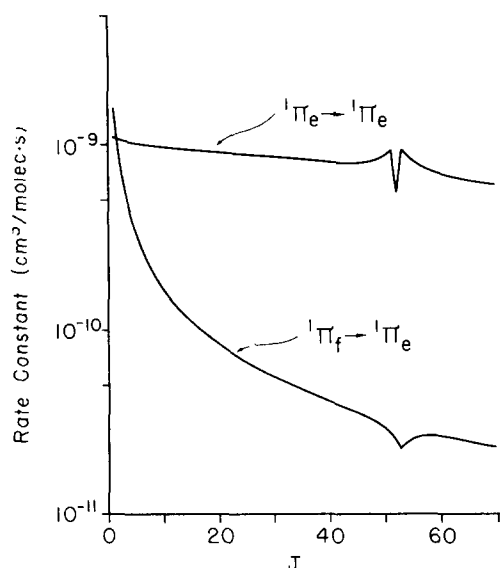
FIG. 8. Rate constants for upward $(J \rightarrow J+1)$ collisional energy transfer within the $v_\Pi = 6$ rotational manifold of the (nominally) $A'\,^1\Pi_e$ state as well as for Q-branch $(\Delta J = 0)$ transfer from the $v_\Pi = 6$, $A'\,^1\Pi_f$ rotational manifold into the $v_\Pi = 6$ rotational manifold of the opposite parity (nominally) $A'\,^1\Pi_e$ state. The slight structure at $J \sim 53$ reflects the mixing between the Born–Oppenheimer $A'\,^1\Pi_e$ and $A\,^1\Sigma^+$ states, which is largest at this isoenergetic point.

(Figs. 4–7), which could be explained by the shorter range of the Ar–CN potential. By contrast, however, Gole and Pace[25] report rate constants of $\sim 1 \times 10^{-7}$ cm^3/molecule s for collisional transfer in ScO from an unassigned reservoir state into the $B\,^2\Sigma^+$ state, also with Ar as a collision partner. These values do seen very large.

Finally, Fig. 8 compares the transfer rates between the different parity Λ-doubled components of the $^1\Pi$ $(v_\Pi = 6)$ rotational manifold with the rates for transfer within the $^1\Pi_e$ manifold. The interparity transitions shown are Q-branch processes $\Delta J_a = 0$; the $^1\Pi_e - ^1\Pi_e$ rates refer to R-branch processes $J_a \rightarrow J_a + 1$. The (nominal) $^1\Pi_e$ rotational levels are of course mixed with levels of the $^1\Sigma^+ (v_\Sigma = 0)$ state. The effect of this mixing explains the nonmonotonic behavior near the isoenergetic point $(J = 52)$. We remember that the $^1\Pi_f$ rotational levels are not mixed with the $^1\Sigma^+$ state. Two observations emerge. First, the rates for rotational relaxation within the (nominal) $^1\Pi_e$ state are somewhat smaller than the comparable rates for rotational relaxation within the (nominal) $^1\Sigma^+$ state (Fig. 4). This reflects the smaller dipole moment within the Born–Oppenheimer $^1\Pi$ state.

A second observation is that the $^1\Pi_f - ^1\Pi_e$ rates drop off rapidly, due to the inverse dependence on J of the reduced matrix elements [Eq. (21)]. Thus, at all but the smallest values of J, $^1\Pi_f - ^1\Pi_e$ transfer is much less probable than the transfer within a Λ-doubling level $(^1\Pi_e - ^1\Pi_e)$. This is consistent with preliminary experimental observations by Pruett and co-workers in the $A'\,^1\Pi$ state of BaO. [64]

It is also worthwhile to examine the rate of transfer from the $^1\Pi_f$ levels into the (nominally) $^1\Sigma^+$ levels. With-

in our assumption of a vanishing $\Sigma-\Pi$ electronic moment [Eq. (79)], this transfer will occur only by virtue of the $^1\Pi_e$ component in the (nominally) $^1\Sigma^+$ state. This component will be largest in the region of the isoenergetic points. In Figs. 4 and 5, we display the resulting rate constants for transfer from, respectively, the $v_\Pi = 6$ and $v_\Pi = 7$ levels of the $A'\,^1\Pi_f$ state into the (nominally) $v_\Sigma = 0$ and $v_\Sigma = 1$ levels of the $A\,^1\Sigma^+$ state by virtue of the mixing of the latter with the $v_\Pi = 6$ and $v_\Pi = 7$ levels of the $A'\,^1\Pi_e$ state. As can be seen, these rates are very small, and will become totally negligible at the higher isoenergetic points due to the falloff of the reduced matrix elements.

VII. DISCUSSION

It is appropriate at this point to examine the possible inaccuracies in our treatment of the energy transfer processes discussed here, and to assess the possible implications of these inaccuracies. First are errors that might be introduced by neglect of terms in the interaction potential other than the dipole–dipole interaction. Certainly, other terms will be present and will play an important role especially at short range. Unfortunately, the dependence on angle and distance of these terms would be accessible only through extensive *ab initio* calculations on the CaO + N$_2$O system, which are unlikely. To judge from our work on rotationally inelastic collisions involving LiH and HF, [38,54,62,65] we feel that inclusion of the shorter range terms would lead to a moderate increase ($\sim 25\%$) in the inelastic cross sections both for rotational relaxation within the (nominally) $^1\Sigma^+$, $^1\Pi$, and $^3\Pi$ manifolds and for transfer between these manifolds. A potentially more important source of error involves the magnitude and sign of $M_{\Sigma\Pi}$, the electronic transition dipole moment between the Born–Openheimer $^1\Pi_e$ and $^1\Sigma^+$ states, which will directly affect the magnitude of the reduced dipole matrix elements [Eqs. (19)–(23)]. Hopefully, these transition moments will be determined and reported in future *ab initio* studies of the excited states of the alkaline earth oxides.

The use of the Born approximation introduces another source of error. On one hand, the predicted cross sections might be inaccurate in magnitude. Also, the rigid rotational selection rules implicit in the reduced dipole matrix elements $(\Delta J = \pm 1$ for $^1\Pi_e \rightleftarrows {}^1\Sigma^+$ transitions, and $\Delta J = 0$ for $^1\Pi_f \rightleftarrows {}^1\Pi_e$ transitions) might not provide a qualitatively accurate description of the true distribution of flux among final rotational states. On the basis of our previous experience with inelastic collisions in polar systems, [38,54,55,62,65] we feel that the considerable averaging which takes place will tend to lessen the impact of this selection rule. Nevertheless, we plan to carry out further determinations of cross sections and rate constants for the CaO + N$_2$O system using the new adiabatically corrected sudden approximation which we have developed. [38,55,56,62] These presumably more accurate values will be a valuable check of the quantitative accuracy of the calculations reported here.

In this paper we have considered separately the non-Born–Oppenheimer mixing between the $^1\Sigma^+$ and $^1\Pi_e$ states and between the $^1\Sigma^+$ and $^3\Pi_{0e}$ states. Ultimately, one should consider the simultaneous mixing between all

three states. However, to first order we expect the population transfer into the (nominally) $^1\Sigma^+$ state from the two Π states to be additive, as will be demonstrated by the following argument: The only non-Born–Oppenheimer coupling between the $^1\Pi$ and $^3\Pi$ states is the spin–orbit term in the full Hamiltonian. Since this couples only states with the same value of Ω, there will be no direct mixing between the two states which feed into the $A\,^1\Sigma^+$ state, namely, $a\,^3\Pi_{0e}$ and $A'\,^1\Pi_e$. Thus, to first order population transfer into the (nominally) $A\,^1\Sigma^+$ state can be treated as two separate two-manifold problems. Of course, one can conceive of a higher order process which involves population transfer from the $^3\Pi_{1e}$ to $^1\Pi_e$ states, which are mixed by the spin–orbit perturbation, followed by the $^1\Pi_e \to {}^1\Sigma^+$ transfer discussed here, or, alternatively, mixing between the $^3\Pi_0$ and $^3\Pi_1$ states followed by $^3\Pi_0 \to {}^1\Sigma^+$ transfer. Neither of these mechanisms was considered further here.

We can use the results of the present study to speculate on the mechanism for collisional transfer of population from dark product states with long radiative lifetimes into the radiating $A\,^1\Sigma^+$ state. We have seen that large transfer rate constants ($k > 1 \times 10^{-10}$ cm^3/molecule s) occur over a relatively narrow range of rotational quantum numbers around the $^1\Pi_e - {}^1\Sigma^+$ and $^3\Pi_{0e} - {}^1\Sigma^+$ isoenergetic points. This transfer is facilitated by the substantial off-diagonal dipole matrix elements which result from the mixing of the Born–Oppenheimer states. The picture which emerges is one of localized windows, through which population transfer occurs. No evidence is seen for a continuous transfer probability, even at very high values of the rotational quantum number. However, due to the fairly high density of isoenergetic points,[66] and due to the fact that the singlet and triplet isoenergetic points alternate (as can be seen by comparison of Figs. 4 and 6 or Figs. 5 and 7), significant transfer rate constants will occur for a large fraction of the rotational levels in each vibrational manifold of the (nominally) $A\,^1\Sigma^+$ state. It is important to remember that only one of the Λ-doubled $^1\Pi$ components and, in the case of the $^3\Pi$ state, only one of the fine-structure components are significantly coupled to the $A\,^1\Sigma^+$ state by collisions. The other Π components will only be accessible reservoir levels through higher order mixing.

Obviously, this picture is limited to CaO, the molecule which was the object of the present calculations. We are currently extending this work to MgO, for which accurate *ab initio* values of the necessary electronic dipole matrix elements are now becoming available,[67] and to BaO, which has been the molecule most studied experimentally. Only then will we have an adequately complete picture of electronic relaxation in the entire alkaline earth oxide family.

We expect then, at least in CaO, that at low to moderate pressure of the oxidant, population transfer will occur at each rotational window by direct dipolar coupling. At higher pressure this process will be augmented by rotational relaxation entirely within the Π states (cf. Fig. 8), which will act to transfer population into these rotational windows. We are now using the rate constants reported here to simulate the pressure dependence of CaO

$A\,^1\Sigma^+ \to X\,^1\Sigma^+$ emission spectra under experimentally realistic conditions.

ACKNOWLEDGMENTS

APPENDIX: MATRIX ELEMENTS OF ELECTRIC MULTIPOLE OPERATOR

The lth electric multipole operator is a spherical tensor of rank l with components given by Eq. (51),[49] which we repeat here:

$$Q_{lm}(\mathbf{r}) = e[4\pi/(2l+1)]^{1/2} \sum_i r_i^l Y_{lm}(\hat{r}_i) \,. \tag{A1}$$

We wish to evaluate matrix elements of Q between molecular state functions, namely,

$$\langle J'\Omega'M'v'S'\Lambda'\Sigma' | Q_{lm} | J\Omega M v S\Lambda\Sigma \rangle \,, \tag{A2}$$

where the components of Q_l refer to a space-fixed frame. The total wave function factors as shown in Eq. (3). Explicitly, the wave function for the electronic and vibrational motion can be written as[44]

$$| vS\Lambda\Sigma \rangle = \chi_v(r)^{2S+1}\phi_\Lambda(\rho, \sigma; r) \,, \tag{A3}$$

where r is the internuclear separation, χ_v the vibrational wave function, ϕ_Λ the electronic wave function, and the coordinates ρ and σ denote collectively the space and spin coordinates of all the electrons, respectively. The coordinates refer here to a molecule-fixed frame.

We define an electronic multipole moment $R_{lq}(r)$ as[68]

$$R_{lq}(r) = \int {}^{2S'+1}\phi_{\Lambda'}(\mathbf{q}, \sigma; r) Q_{lq}(\mathbf{q}, r)^{2S+1}\phi_\Lambda(\mathbf{q}, \sigma; r) d\mathbf{q}\, d\sigma \,, \tag{A4}$$

where the components of the operator Q refer now to the molecule-fixed frame. In fact, since the overall dependence of the electronic wave function on the azimuthal angle is $\exp(i\Lambda\phi)$,[69] and since the electric multipole operator is independent of spin, it is easy to show that the only nonvanishing component of the electric multipole moment is the one for which $m = \Lambda' - \Lambda$. Also, the spin selection rules $\Delta S = \Delta\Sigma = 0$ must be satisfied. Subsequent vibrational averaging yields a transition multipole moment

$$Q_{v'v}^{l; \Lambda'-\Lambda} = \int \chi_{v'}(r) R_{l, \Lambda'-\Lambda}(r) \chi_v(r) dr \,, \tag{A5}$$

which could be simplified within the Franck–Condon approximation to yield

$$Q_{v'v}^{l,\Lambda'-\Lambda} \simeq R_{l,\Lambda'-\Lambda}(r_e)\langle \chi_{v'}|\chi_v\rangle . \tag{A6}$$

It is now necessary to integrate over the wave function or the rotating molecule, namely,[44]

$$|J\Omega M\rangle = [(2J+1)/8\pi^2]^{1/2} D_{M\Omega}^{J*} \tag{A7}$$

where $D_{M\Omega}^{J}$ is a rotation matrix element and where the definition of the Euler angles is that of Brink and Satchler.[70] Since these angles refer to the space-fixed frame, it is necessary to convert the $Q_{v'v}^{l,\Lambda'-\Lambda}$ component into the space frame as follows:

$$^{SF}Q_{v'v}^{lm} = D_{m,\Lambda'-\Lambda}^{l*} Q_{v'v}^{l,\Lambda'-\Lambda} . \tag{A8}$$

Note that there is no summation on the right-hand side of Eq. (A8) because there is only one nonvanishing molecule frame component.

Finally, the matrix elements (A2) can be expressed as

$$\langle J'\Omega'M'v'S'\Lambda'\Sigma'|Q_{lm}|J\Omega MvS\Lambda\Sigma\rangle = \delta(S,S')\delta(\Sigma,\Sigma') Q_{v'v}^{l,\Lambda'-\Lambda}$$

$$\times \frac{[(2J+1)(2J'+1)]^{1/2}}{8\pi^2} \int D_{M'\Omega'}^{J'} D_{q,\Lambda'-\Lambda}^{l*} D_{M\Omega}^{J*} d\Omega . \tag{A9}$$

Using the known expression for the integral over three rotation matrix elements and the known symmetry properties of the $3j$ symbols,[49] we can write Eq. (A9) in factorized form[50]:

$$\langle J'\Omega'M'v'S'\Lambda'\Sigma'|Q_{lm}|J\Omega MvS\Lambda\Sigma\rangle$$

$$= \delta(S,S')\delta(\Sigma,\Sigma')(-1)^{J'-M'}\begin{pmatrix} J' & l & J \\ -M' & m & M \end{pmatrix}$$

$$\times (J'\Omega'v'S'\Lambda'\Sigma'||Q_l||J\Omega vS\Lambda\Sigma) , \tag{A10}$$

here the reduced matrix element is

$$(J'\Omega'v'S'\Lambda'\Sigma'||Q_l||J\Omega vS\Lambda\Sigma)$$

$$= (-1)^{J'-\Omega'}Q_{v'v}^{l,\Lambda'-\Lambda}$$

$$\times [(2J+1)(2J'+1)]^{1/2}\begin{pmatrix} J' & l & J \\ -\Omega' & \Lambda'-\Lambda & \Omega \end{pmatrix} . \tag{A11}$$

If, finally, the molecular eigenfunctions are linear combinations of Hund's case (a) functions, then the expectation value of the multipole operator can still be written in factorized form [Eq. (A10)], except that the reduced matrix elements will be linear combinations of the reduced matrix elements between the various component states [Eq. (A11)].

[1]C. D. Jonah, R. N. Zare, and Ch. Ottinger, J. Chem. Phys. 56, 263 (1972); A. Schultz and R. N. Zare, ibid. 60, 5120 (1974); F. Engelke, R. K. Sander, and R. N. Zare, ibid. 65, 1416 (1976).

[2]C. R. Dickson, S. M. George, and R. N. Zare, J. Chem. Phys. 67, 1024 (1977).

[3]D. J. Wren and M. Menzinger, J. Chem. Phys. 63, 4557 (1975); Faraday Discuss. Chem. Soc. 67, 97 (1979).

[4]A. Siegel and A. Schultz, Chem. Phys. 28, 265 (1978).

[5]P. J. Dagdigian, Chem. Phys. Lett. 55, 239 (1978); B. E. Wilcomb and P. J. Dagdigian, J. Chem. Phys. 69, 1779 (1978); L. Pasternack and P. J. Dagdigian, Chem. Phys. 33, 1 (1978).

[6]J. A. Irvin and P. J. Dagdigian, J. Chem. Phys. 73, 176 (1980).

[7]J. A. Irvin and P. J. Dagdigian, J. Chem. Phys. 74, 6178

[8]J. A. Irvin and P. J. Dagdigian (unpublished).

[9]C. R. Jones and H. P. Broida, J. Chem. Phys. 60, 4369 (1974).

[10]C. R. Jones and H. P. Broida, J. Chem. Phys. 59, 6677 (1973).

[11]R. W. Field, C. R. Jones, and H. P. Broida, J. Chem. Phys. 60, 4377 (1974).

[12]B. G. Wicke, M. A. Revelli, and D. O. Harris, J. Chem. Phys. 63, 3120 (1975).

[13]G. A. Capelle, C. R. Jones, J. Zorski, and H. P. Broida, J. Chem. Phys. 61, 4777 (1974).

[14]A. Torres-Filho and J. G. Pruett, J. Chem. Phys. 70, 1427 (1979); A. Torres-Filho and J. G. Pruett, J. Chem. Phys. (in press).

[15]D. J. Benard, W. D. Slafer, and J. Hecht, J. Chem. Phys. 66, 1013 (1977).

[16]D. J. Benard and W. D. Slafer, J. Chem. Phys. 66, 1017 (1977); D. J. Benard, W. D. Slafer, and P. H. Lee, Appl. Opt. 16, 2108 (1977).

[17]D. J. Eckstrom, S. A. Edelstein, D. L. Huestis, B. E. Perry, and S. W. Benson, J. Chem. Phys. 63, 3828 (1975); D. J. Eckstrom, J. R. Barker, J. G. Hawley, and J. P. Reilly, Appl. Opt. 16, 2102 (1977).

[18]C. J. Hsu, W. D. Krugh, and H. B. Palmer, J. Chem. Phys. 60, 5118 (1974).

[19]E. S. Fleming and H. B. Palmer, in Electronic Transition Lasers, edited by J. I. Steinfeld (M.I.T., Cambridge, Mass. 1976), p. 70.

[20]R. W. Field, R. A. Gottscho, J. G. Pruett, and J. J. Reuther, "Barium Oxide: The Question Unanswered," in Proceedings of the 14th International Conference on Free Radicals, Sanda, Japan (1979).

[21]R. W. Field, J. Chem. Phys. 60, 2400 (1974).

[22]K. P. Huber and G. Herzberg, Constants of Diatomic Molecules (Van Nostrand Reinhold, New York, 1979).

[23]Throughout this paper we shall use the spectroscopic state labels appropriate to CaO, the molecule which is the subject of our numerical calculations, namely, $a^3\Pi$, $A'^1\Pi$, $b^3\Sigma^+$, and $A^1\Sigma^+$. For the other alkaline earth oxides the spectroscopic labels occasionally differ. In particular, for MgO the four excited states are denoted $a^3\Pi$, $A^1\Pi$, $b^3\Sigma^+$, and $B^1\Sigma^+$ (Ref. 22); and, for BaO, $a^3\Sigma^+$, $A^1\Sigma^+$, $b^3\Pi$, and $A'^1\Pi$ [R. A. Gottscho, J. Chem. Phys. 70, 3554 (1979)].

[24]M. J. Sayers and J. L. Gole, J. Chem. Phys. 67, 5442 (1977); A. W. Hanner and J. L. Gole, ibid. 73, 5025 (1980).

[25]J. L. Gole and S. A. Pace, J. Chem. Phys. 73, 836 (1980).

[26]D. H. Katayama, T. A. Miller, and V. E. Bondybey, J. Chem. Phys. 71, 1662 (1979).

[27]V. E. Bondybey and T. A. Miller, J. Chem. Phys. 69, 3602 (1978); D. H. Katayama, T. A. Miller, and V. E. Bondybey, ibid. 72, 5469 (1980).

[28]R. G. Gordon and Y. N. Chiu, J. Chem. Phys. 55, 1469 (1971).

[29]Y. N. Chiu, J. Chem. Phys. 55, 5052 (1971).

[30]S. H. Lin, Mol. Phys. 21, 853 (1971); Proc. R. Soc. London Ser. A 335, 51 (1973).

[31]K. N. Klump and E. N. Lassettre, J. Chem. Phys. 68, 886 (1978).

[32]R. A. Gottscho, J. B. Koffend, and R. W. Field, J. Mol. Spectrosc. 82, 310 (1980).

[33]J. M. Brown, J. T. Hougen, K. P. Huber, J. W. C. Johns, I. Kopp, H. Lefebvre-Brion, A. J. Merer, D. A. Ramsay, J. Rostas, and R. N. Zare, J. Mol. Spectrosc. 55, 500 (1975).

[34]C. G. Gray and J. Van Kranendonk, Can. J. Phys. 44, 2411 (1966).

[25]H. A. Rabitz and R. G. Gordon, J. Chem. Phys. 53, 1815, 1831 (1970).

[36]R. D. Sharma and C. A. Brau, J. Chem. Phys. 50, 924 (1969).

[37] For an excellent review, see G. G. Balint-Kurti, in *International Review of Science, Physical Chemistry* (Butterworth, London, 1975), Series 2, Vol. 1.

[38] P. J. Dagdigian and M. H. Alexander, J. Chem. Phys. **72**, 6513 (1980).

[39] M. Shapiro and H. Kaplan, J. Chem. Phys. **71**, 2182 (1979).

[40] R. N. Dixon and D. Field, Proc. R. Soc. London Ser. A **366**, 225 (1979), **368**, 99 (1979).

[41] D. P. Dewangan and D. R. Flower, J. Phys. B **14**, 2179 (1981).

[42] M. H. Alexander and D. Misra, Abstract, 8th ACS–MARM Meeting, Washington, D. C. (1973); Bull. Am. Phys. Soc. **18**, 687 (1973); D. Misra, Ph. D. thesis, Department of Physics, University of Maryland, 1974.

[43] J. T. Hougen, Nat. Bur. Stand. U. S. Monogr. **115** (1970).

[44] R. N. Zare, A. L. Schmeltekopf, W. J. Harrop, and D. L. Albritton, J. Mol. Spectrosc. **46**, 37 (1973).

[45] The curves in Fig. 1 were determined using the presumably deperturbed spectroscopic constants (ω_e, B_e, T_e; Ref. 21). Thus, the curves are virtually equivalent to the Born–Oppenheimer energies.

[46] R. A. Gottscho, J. B. Koffend, R. W. Field, and J. R. Lombardi, J. Chem. Phys. **68**, 4110 (1978).

[47] Y. C. Hsu, B. Hegemann, and J. G. Pruett, J. Chem. Phys. **72**, 6437 (1980).

[48] C. G. Gray, Can. J. Phys. **54**, 505 (1976).

[49] A. R. Edmonds, *Angular Momentum in Quantum Mechanics* (Princeton University, Princeton, 1960).

[50] Our definition of the reduced matrix element follows Eq. (5.4.1) of Ref. 49.

[51] For a related discussion of the experimental determination (in the SrF molecule) of the relative signs of dipole-moment and orbit–rotation matrix elements, see J. Nakagawa and D. O. Harris, J. Mol. Spectrosc. **86**, 65 (1981).

[52] At first glance Eq. (48) differs from standard expressions (Refs. 29, 34–36, and 48) but may be easily shown to be entirely equivalent if Eqs. (49)–(52) are substituted into Eq. (4

[53] R. J. Cross, Jr. and R. G. Gordon, J. Chem. Phys. **43**, 3571 (1966).

[54] A. E. DePristo and M. H. Alexander, J. Chem. Phys. **66**, 1334 (1977).

[55] M. H. Alexander and A. E. DePristo, J. Phys. Chem. **83**, 1499 (1979).

[56] M. H. Alexander, J. Chem. Phys. **71**, 1683 (1979).

[57] R. D. Nelson, D. R. Lide, Jr., and A. A. Maryott, Natl. Stand. Ref. Data Ser., Natl. Bur. Stand. **10** (1967).

[58] G. Herzberg, *Infrared and Raman Spectra of Polyatomic Molecules* (Van Nostrand, Princeton, 1968).

[59] W. England, Chem. Phys. **53**, 1 (1980).

[60] C. W. Bauschlicher, Jr. and D. R. Yarkony, J. Chem. Phys. **68**, 3990 (1978).

[61] R. G. Parr, *Quantum Theory of Molecular Electronic Structure* (Benjamin, New York, 1963), p. 26.

[62] P. J. Dagdigian, B. E. Wilcomb, and M. H. Alexander, J. Chem. Phys. **71**, 1670 (1979).

[63] R. A. Gottscho, R. W. Field, R. Bacis, and S. J. Silvers, J. Chem. Phys. **73**, 599 (1980).

[64] J. G. Pruett (private communication, 1981).

[65] M. H. Alexander, J. Chem. Phys. **73**, 5135 (1980).

[66] The location of the $^1\Pi_e$–$^1\Sigma^+$ and $^3\Pi_{0e}$–$^1\Sigma^+$ isoenergetic points can be seen in Figs. 4–7.

[67] C. W. Bauschlicher, Jr. and D. R. Yarkony (work in progress, 1981).

[68] The notation follows that of F. E. Whiting, A. Schadee, J. B. Tatum, J. T. Hougen, and R. W. Nicholls, J. Mol. Spectrosc. **80**, 249 (1980).

[69] See, for example, S. Green and R. N. Zare, Chem. Phys. **7**, 62 (1975).

[70] D. M. Brink and G. R. Satchler, *Angular Momentum* (Oxford University, Oxford, 1975), 2nd edition.